Received: 28 September 2023 | Accepted: 27 March 2024 | Published online: 30 July 2024

DOI: 10.1002/saj2.20695

Soil Science Society of America Journal

ORIGINAL ARTICLE

Fundamental Soil Science

Spodosol development and soil organic carbon distribution along a lithosequence in perhumid coastal temperate rainforest

Jennifer Fedenko[1] | **David D'Amore**[2] | **Diogo Spinola**[2,3] | **Raquel Portes**[4] | **Ashlee Dere**[5] | **Rebecca A. Lybrand**[1]

[1]Department of Crop and Soil Science, Oregon State University, Corvallis, Oregon, USA

[2]USDA Forest Service, Pacific Northwest Research Station, Juneau, Alaska, USA

[3]Department of Chemistry and Biochemistry, University of Alaska Fairbanks, Fairbanks, Alaska, USA

[4]Department of Earth and Climate Sciences, Bates College, Lewiston, Maine, USA

[5]Department of Geography/Geology, University of Nebraska, Omaha, Nebraska, USA

Correspondence
Rebecca Lybrand, Department of Land, Air & Water Resources, University of California, Davis, One Shields Avenue, Davis, CA 95616, USA.
Email: ralybrand@ucdavis.edu

Assigned to Associate Editor Kyungsoo Yoo.

Present addresses
Diogo Spinola, Department of Ecosystem Science and Management, University of Northern British Columbia, Prince George, British Columbia, Canada.

Raquel Portes, Department of Geography, Earth and Environmental Sciences, University of Northern British Columbia, Prince George, British Columbia, Canada.

Rebecca A. Lybrand, Department of Land, Air & Water Resources, University of California, Davis, Davis, Callifornia, USA.

Funding information
Pacific Northwest Research Station, Grant/Award Number: 19JV11261933084; National Science Foundation, Grant/Award Number: 2131432

Abstract

A dense concentration of old-growth forest and a wet, cold climate promote mineral weathering and leaching in coastal temperate rainforest soils. Our objective was to assess soil development and soil organic carbon (SOC) distribution across 18 soil profiles in remote, upland terrain of southeast Alaska where pedon data are sparse. We made soil morphological observations, collected samples, and completed laboratory analyses to measure SOC content, pH, and particle size distribution. The survey of upland backslope soils included north- and south-facing hillslopes derived from three lithologies (slate, metavolcanic, and phyllite). The soils across all sites were very gravelly (51.8 ± 20.4% coarse fragments), acidic (mineral soil pH 4.85 ± 0.45), and moderately deep (96.56 ± 37.80 cm); thin, broken E horizons were underlain by thick, carbon-rich spodic horizons. Soil development was relatively consistent as demonstrated by the Profile Development Index with values from 15 to 26 and Podzolization Index values spanning 8 to 14. A mean pedon SOC stock of 198.02 ± 81.42 Mg C ha^{-1} (n = 18) was calculated using data collected for all upland organic and mineral soils from our work. The accumulation of SOC was similar among soils formed from contrasting lithologies with averages of 182 ± 15.70 Mg C ha^{-1} for slate, 188 ± 53.80 Mg C ha^{-1} for metavolcanic, and 218 ± 124 Mg C ha^{-1} for phyllite. Our work contributes to soil morphological observations, laboratory data, and SOC stock estimates required to better constrain and model pedogenic processes and SOC stock in remote forests where data sets are limited.

Abbreviations: MAP, mean annual precipitation; MAT, mean annual temperature; NPCTR, northeast pacific coastal temperate rainforest; NRCS, Natural Resources Conservation Service; PDI, Profile Development Index; PNW, Pacific Northwest; POD, Podzolization Index; PSA, particle size analysis; SOC, soil organic carbon.

1 | INTRODUCTION

The coastal rainforests of the Pacific Northwest (PNW) contain some of the world's oldest trees (DellaSala et al., 2011) where soils accumulate over half of the total organic carbon in the system (Carpenter et al., 2014; Leighty et al., 2006; Smithwick et al., 2002). The carbon-dense soils support mineral transformation processes that release plant essential nutrients belowground, host root networks that cycle nutrients and transport water, provide a foundation for forests which in turn sustain wildlife via food and shelter, and contribute to other ecosystems services such as recreation and heritage preservation (Keith et al., 2009; Lin, 2012; Smithwick et al., 2002). Yet, research gaps remain in understanding soil genesis and carbon accumulation in upland coastal rainforest soils when compared to boreal, permafrost, and other temperate forest soils (Carpenter et al., 2014; Lin, 2012). The forest soil pedon data required to train predictive models of SOC stock and nutrient cycling are also limited spatially and sparse numerically relative to agricultural landscapes due to limitations in accessing remote forested regions (Blackford et al., 2020; Soil Survey Staff, 2022). Here, we examine soil development and the distribution of soil organic carbon (SOC) in soils derived from contrasting parent materials across well-drained, upland positions in Alaska's perhumid coastal temperate rainforest.

The Tongass National Forest covers 8.5 million ha of southeast Alaska, serves as the largest national forest in the United States, and spans the northernmost perhumid sub-region of the Northeast Pacific Coastal Temperate Rainforest (NPCTR; Carstensen et al., 2007). This region supports one of the largest and most intact areas of old growth forest in the world (Carstensen et al., 2007; Leighty et al., 2006) where forest carbon has been identified as a net sink (U.S. Forest Carbon Data, 2023). Approximately 66% of the carbon in the Tongass persists in the soil compared to 30% in aboveground biomass (Leighty et al., 2006). Only 60% of the land area in the administrative unit of the Tongass National Forest has correlated soil maps associated with the description and sampling of pedons despite the high proportion of carbon allocated belowground (USDA Forest Service, 2016). The mapped regions do not contain the detailed information required to understand SOC dynamics, particularly information on how soil properties may impact SOC distribution, persistence, and fluxes across the landscape. Prior research and mapping activities in the Tongass have found that the NPCTR uplands are dominated by shallow-to-deep mineral soils that classify as Spodosols (Alexander et al., 1989), which are soils that contain abundant SOC with a complex array of organo-mineral bonding pathways facilitated by leaching and translocation processes (Johnson et al., 2011; Kögel-Knabner & Amelung, 2021; Schaetzl & Isard, 1991; Stone et al., 1993). The complex nature of organo-mineral associations in soil contributes

Core Ideas

- Well-developed Spodosols formed on steep backslopes in upland landscapes of Alaskan coastal temperate rainforests.
- Soil organic carbon (SOC) accumulated consistently across 18 soil profiles formed from contrasting parent materials.
- A greater proportion of SOC was found in mineral soils versus overlying organic horizons.
- Almost 40% of SOC would not be accounted for if sampling had been restricted to the upper 30 cm of the soil.

to a great deal of uncertainty in the persistence and distribution of SOC (Kleber et al., 2021) as does the composition and transformation of organic matter distributed vertically in Spodosols (Brock et al., 2020; Krettek et al., 2020).

One of the key challenges for assessing pedogenic processes and SOC distribution involves identifying the drivers of variability across space, time, and scales, particularly at localized levels (i.e., molecular, pedon, and landscape; Kleber et al., 2021; Nave et al., 2021). Most SOC in forests accumulates in subsurface mineral horizons that occur at depths greater than 20 cm (Harrison et al., 2011; James et al., 2014; Rumpel & Kögel-Knabner, 2011). The eluviation-illuviation of organo-mineral complexes and retention of dissolved organic carbon through the association with reactive minerals, such as Al and Fe oxyhydroxides, are the main mechanisms responsible for subsurface C enrichment in Spodosols (Heckman et al., 2018; Kalbitz et al., 2000; Kögel-Knabner et al., 2008). Similar observations have been made for SOC distribution in Spodosols from the NPCTR in Alaska where recent work suggests that mineral weathering products, including concentrations of Fe-Al oxyhydroxide concentrations, may be influenced by site-specific properties including lithology (i.e., Spinola et al., 2022).

Texture, bulk density, mineralogical composition, secondary weathering products, among other soil properties in Spodosols often vary with lithology and influence the properties associated with SOC accumulation (Schaetzl & Thompson, 2015). Examining soil formation and SOC distribution in soils of the same order yet developed from different lithologies can provide a more refined understanding of the most prevalent soil forming factors in forested ecosystems. One study found that seven Spodosols in the NPCTR derived from contrasting parent rock, that is, basalt and limestone, were relatively homogenous with respect to soil morphology and physicochemical properties (Heilman & Gass, 1974). Recent work near Juneau, Alaska, found that Spodosols formed along a lithosequence presented similar morphological properties yet differed in the degree of weathering and the concentrations of Fe-Al oxyhdroxides (Spinola et al., 2022). Both studies attributed the relatively homogenous soil properties to the combined influence of the perhumid climate and high organic matter inputs that promoted rapid rates of podzolization (Alexander & Burt, 1996; Burt & Alexander, 1996). Interestingly, the findings from Spinola et al. (2022) suggested that the capacities and mechanisms by which soils accumulate carbon may be influenced by properties imparted by contrasting bedrock types.

Questions remain in understanding variations in soil development, SOC spatial distribution, and soil depth in upland Spodosols from the NPCTR (e.g., Johnson et al., 2011); this uncertainty is therefore imparted to spatially predictive models for soil carbon and nutrient cycling that can only be improved by employing coordinated field sampling campaigns that examine soil development and capture the variability of soil–landscape associations. The extensive distribution of SOC in the Spodosols of the NPCTR has been documented (i.e., McNicol et al., 2019). However, to date, there has been little focused replication of pedons across upland forested landscapes in the NPCTR. Our work asks the following questions: how does the development of upland mineral soils vary within the NPCTR as quantified using established indices, such as the Profile Development Index (PDI) or the Podzolization Index (POD) (Harden, 1982; Harden & Taylor, 1983; Schaetzl & Mokma, 1988)? And how does the distribution of SOC differ with depth or between mineral and organic soil horizons?

The objectives of our study were to (1) perform soil morphological assessments of Spodosols formed under an intense weathering regime in cold, wet temperate rainforest environments; (2) quantify the degree of soil development in the upland soil environments using the PDI and the POD; and (3) examine the subsurface accumulation and distribution of SOC across a range of upland backslope soils subject to existing temperature and precipitation patterns. We hypothesized that soils derived from contrasting lithologies would present notable differences in soil development as a result of different weathering pathways (i.e., higher PDI and POD values in more well-developed soils according to Harden [1982], Harden and Taylor [1983], and Schaetzl and Mokma [1988]). We also predicted that SOC content would be highest in the soils with the most well-expressed Spodosols as indicated by the POD. Here, we described, sampled, and analyzed soils collected from 18 soil profiles in upland landscapes of old-growth temperate rainforest near Juneau, AK. The survey included soils from north- and south-facing hillslopes derived from three distinct rock types (metavolcanic, slate, and phyllite) that represent key metasedimentary assemblages associated with broader island arc geology or geologically active coastal margins (Gehrels, 2001). Our study provides an assessment of soil formation in complex upland terrain from the coastal margin of southeast Alaska (USDA Forest Service, 1996), which is translatable to other temperate rainforest systems in western North America. We contribute to a growing body of pedon data required to better inform and constrain nutrient cycling and terrestrial carbon models.

2 | MATERIALS AND METHODS

2.1 | Study area

We established a sequence of sites in the perhumid coastal temperate rainforest (PCTR), which falls within the Northeast Pacific Coastal Temperate Rainforest (NPCTR) and spans the coastal edge from British Columbia to southeast Alaska (Figure 1; Table A1). The climate associated with our field sites near Juneau, Alaska, is cool and wet with a mean annual temperature of 5.6˚C, mean annual precipitation of 1582 mm, and mean annual snowfall of 2202 mm (ACRC, 2020). The soil moisture regime is perudic (Alexander, 1990; Alexander & Burt, 1996) indicating that soils remain moist throughout the year because the large volume of precipitation exceeds evapotranspiration (Soil Survey Staff, 2014). Soil drainage classes range from moderately well drained to well drained (Soil Survey Staff, 2014). The forests typically occur on steep slopes with well-drained soils with a distinct hummocky microtopography and varying thickness of the soil organic horizon. All of the field areas occur within the same vegetation category of "Closed Western Hemlock-Sitka Spruce (Western Redcedar) Forest" (Viereck et al., 1992) with vegetation types that are climax successional communities. Western hemlock (*Tsuga heterophylla*) is most dominant while Sitka spruce (*Picea sitchensis*) co-dominates at a lower abundance than Western hemlock. Other less dominant tree species include mountain hemlock (*Tsuga mertensiana*) and Sitka alder (*Alnus rubra*; Heusser, 1960). Western Redcedar was absent within our field areas and is more prevalent further south in the forest category range. The understory has a well-developed shrub layer with 1–1.5 m tall shrubs. The understory is predominantly composed of blueberry (*Vaccinium alaskaense*), oval-leaved blueberry (*Vaccinium ovalifoium*), rusty menziesia (*Menziesia ferruginea*), and devil's club (*Oplopanax horridum*), with abundant forbs and mosses covering the forest floor including *Rhytidiadelphus* and *Hylocomium* ssp. (Heilman & Gass, 1974).

2.2 | Geologic setting

The soils developed from colluvial deposits of rocks belonging to the Taku terrane and Gravina belt deposits, which were

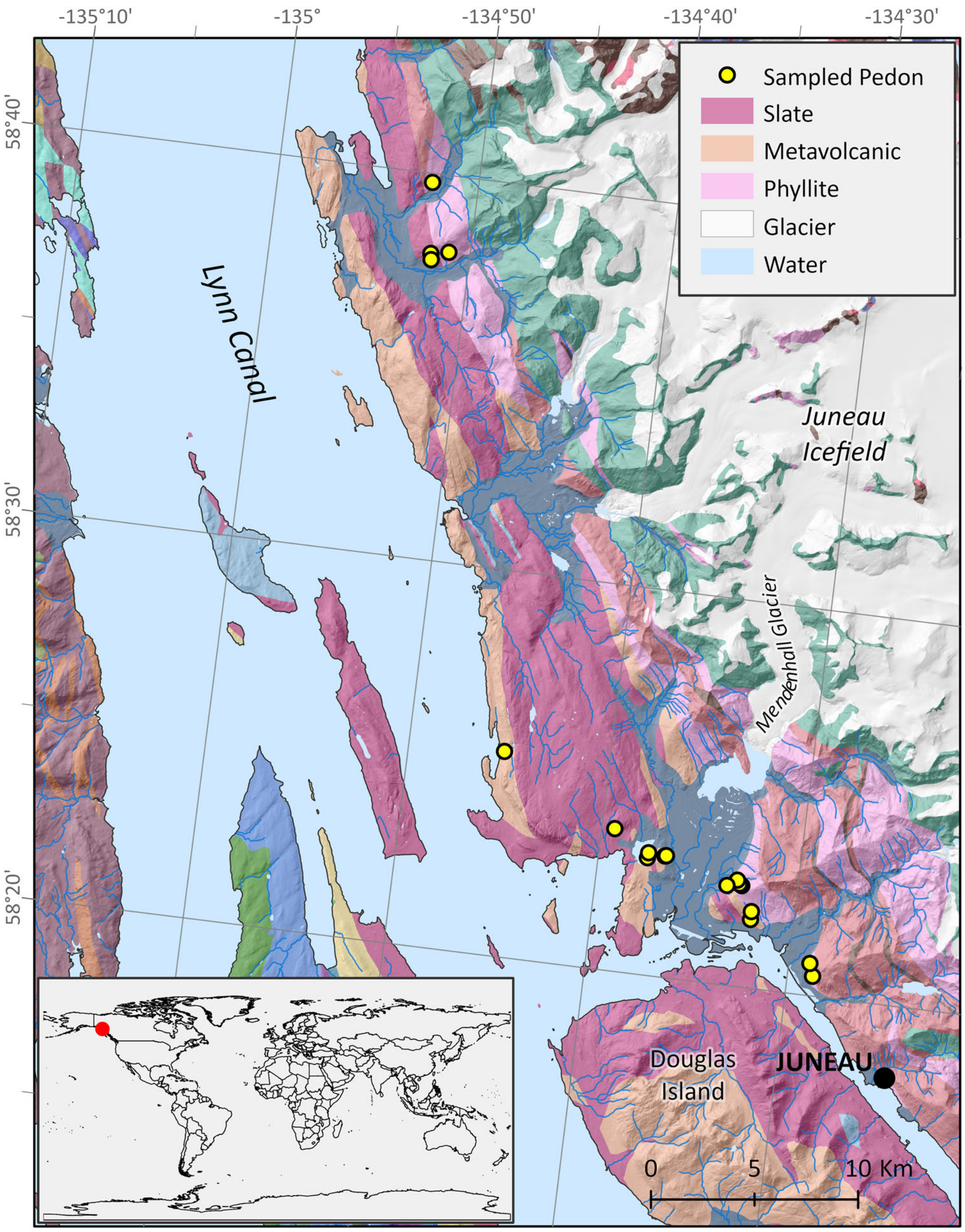

FIGURE 1 Overview site map of the perhumid coastal temperate rainforest field area located near Juneau, Alaska, including the geologic setting for the 18 soil profiles sampled in the study. Inset maps for each field area are available in Figure A1.

adhered to the North American continent as accreted terranes through tectonic plate movement (Gehrels, 2001; Gehrels & Berg, 1994; Stowell, 1990). The geology of southeast Alaska is complex and composed of heterogeneous tectonic assemblages that gradually metamorphose in an easterly direction, toward the Coast Mountains batholith of intrusive igneous rock (Berg et al., 1972; Ford & Brew, 1987; Gehrels & Berg H.C., 1994).

Low-grade metamorphic rocks (greenschist facies) with different protoliths are prevalent in the study area (Berg et al., 1972; Ford & Brew, 1987). The geologic units have a distinct southeast to northwest trend in their orientation and occur adjacent to one another on the landscape (Figure 1).

Our survey of upland soil profiles included north-facing and south-facing soils formed from slate, metavolcanic, and phyllite lithologies. The metavolcanic lithology is basaltic in composition (McClelland et al., 1992), with a mineralogical assemblage comprising albite, amphibole (actinolite), chlorite, muscovite, epidote, and pyroxene (Spinola et al., 2022). The phyllite and slate lithologies are similar with respect to mineralogical composition and include quartz, chlorite, muscovite, biotite, and albite (Spinola et al., 2022). Phyllite exhibited larger grain sizes when compared to the slate in combination with a marked preferential orientation of mica, which presented a reflective sheen that was not visible on the slate (Spinola et al., 2022).

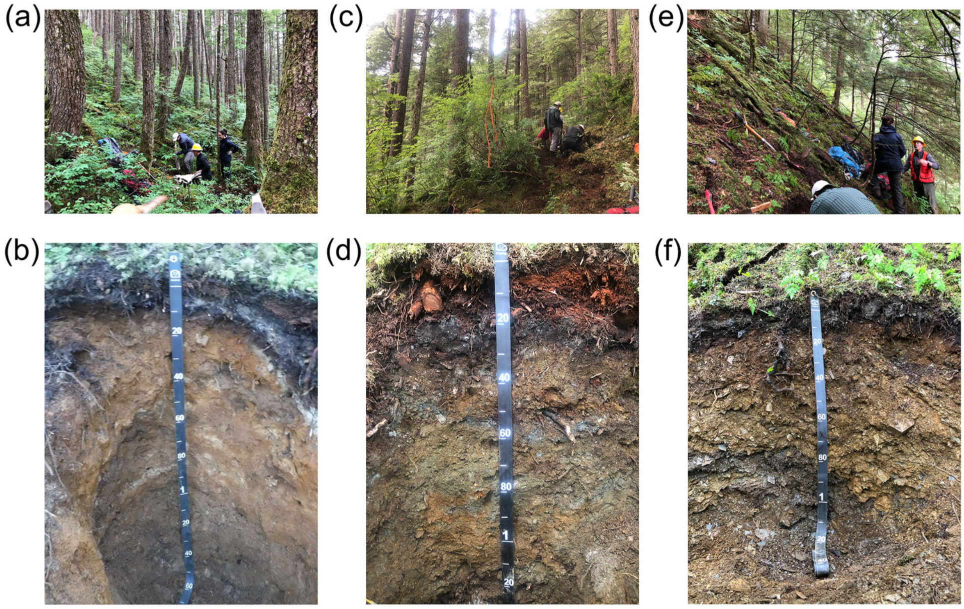

FIGURE 2 Landscape level photographs showing the steep backslope positions and accompanying soil profile photos for each lithology type in the study represented from left to right: (a and b) metavolcanic (P20), (c and d) phyllite (P8), and (e and f) slate (P13). Soil morphological observations and horizon designations for each soil are available in Table A2.

2.3 | Site selection and sampling

We sampled 18 soil profiles from backslope positions on forested hillslopes from each of the three most prominent lithologies (Figures 1 and 2; Figure A1; Table A1). The hillslopes were characterized by short slope lengths, ~150 m from the summit to mid backslope positions. The slopes are generally convex with a gradient from 31% to 80% (USDA, 1996). We specifically selected soils from backslope positions at ~200 m in elevation on each hillslope to ensure that samples were collected above the till line to avoid glacial till deposits. Between ~15 and 13ka, southeast Alaska was ice-free, following the retreat of the Cordilleran Ice Sheet (Baichtal et al., 2021). The slopes from which the soils were collected did not show evidence of Pleistocene till deposits above a certain altitude threshold. The "till line" consists of poorly drained glacial deposits (mostly glaciofluvial outwash deposits and glaciomarine deposits) that serve as parent material for Cryaquods and Cryohemists (D'Amore et al., 2015). The soils analyzed in our study formed from the redistribution of colluvial material derived from fracturing rock and eroded material from upper slopes of the field areas that was then deposited on mid-slope landscape positions. As noted in most profiles, there was no till evident in the pedons, and mineralogical analyses have confirmed that the symmetry of the sediments and soils coincide with the varying bedrock types (Spinola et al., 2022). Overall, we did not observe any very poorly sorted or mixed glacial deposits as parent material within the backslope positions of our specific field areas; there were also no remnants of paleosols or evidence for early Pleistocene soil development.

The Spodosols sampled here were derived from colluvial deposits that also do not resemble the Central European Cover beds (i.e., Semmel & Terhorst, 2010), which exhibit periglacial features such as ice wedges, cryoturbation structures, high bulk density, and the presence of loess. The parent material of the sampled soils was composed of lithologically homogeneous colluvial deposits, likely formed after the retreat of the ice cover. However, the region's steep slopes also contribute to modern-day colluvial processes, such as mass wasting.

Of the 18 soil pedons examined, 11 pedons were sampled from south-facing hillslopes and seven from north-facing positions (Figures 1 and 2; Tables A1 and A2). The soils were described and sampled by pedogenic horizon from sites derived from colluvial parent material and excavated to a depth of ~1 m or to the refusal of parent material contact where it was physically prohibitive to dig further. We identified soil morphological horizons and described color, structure, texture, stickiness, root and pore abundance, and rock fragment percentages according to protocols from the Natural Resources Conservation Service (NRCS; Schoeneberger et al., 2012/2021). Bulk soil samples and select rock samples were collected for all soil profiles. Bulk density samples for the mineral soils were also sampled using a soil volumetric core with two replicates collected from each horizon. The bulk density for organic horizons was measured by sampling 5 cm^3 sized cubes that were weighed, oven-dried, with a final mass then divided by 125 cm^3.

Soil samples were air-dried and sieved to <2 mm to represent the fine-earth fraction required for analysis (Soil Survey Staff, 2014). Rock fragment percent (≥2 mm) was also quantified (Soil Survey Staff, 2014). Soils were subsampled for organic carbon and nitrogen analysis, bulk density, pH, and particle size distribution. The remaining samples were archived at the Pacific Northwest Research Station Forestry Sciences Laboratory in Juneau, Alaska.

2.4 | Laboratory analysis

Samples were ground to ≤180 μm using a Retsch Mixer Mill 400 with 10 mm tungsten carbide balls in a 25-mL tungsten carbide grinding vessel. Total carbon and nitrogen content were determined at Oregon State University's Soil Health Laboratory using an Elementar Vario MACRO Cube that measures CO_2, N_2, and SO_2 by utilizing combustion at a temperature of 1150˚C. We assumed that total C and N equate to organic C and N as we did not detect carbonates in our samples. Organic C and N percentages are presented on an oven-dry basis. Mineral soil (80 mg) and organic soil (40 mg) were wrapped in 35 mm × 35 mm tin foil and analyzed. Soil carbon and nitrogen stocks were calculated for each horizon and summed for each pedon.

Soil carbon stocks C_i (Mg ha^{-1}) for the ith horizon were calculated using the following equation (Rasmussen, 2006; Tan et al., 2004):

$$C_i = D_b\, Z_i\, (1 - Vr)\, C, \tag{1}$$

where D_b is the bulk density, Z_i is the thickness of the ith horizon, Vr is the volumetric rock fragment content calculated from weight percent of rock >2 mm (Torri et al., 1994), and C is the percent carbon. When determining soil carbon stocks, if bulk density or volumetric rock fragments were unavailable, averages were calculated from the same soil horizons and from sites with the same lithology. Rock fragment density was assumed to be 2.65 g/cm^3 (Sharma, 1997).

Soil pH was measured for each horizon using an Accumet AP72 pH meter. A ratio of 1:1 water to soil was used for pH extractions except for organic horizons where a 2:1 or 4:1 water to organic matter ratio was used to ensure sample contact with the pH probe. Ten grams of soil was mixed with 10 mL of water, stirred initially, and stirred again after 10 and 20 min. Atmospheric temperature was recorded for each pH measurement (Soil Survey Staff, 2014).

Samples collected for bulk density measurements of the mineral horizons were sampled with a soil volumetric core (138.5 cm^3), weighed, and estimated using the intact core method (Soil Survey Staff, 2014). To calculate bulk density, soil samples were oven dried and rock fragments were sieved (>2 mm) out after drying. The soils were then weighed, and the mass was divided by the volume of the soil volumetric core (138.5 cm^3).

Particle size analysis (PSA) was determined using the sieve and pipette method by the Soil Health Laboratory at Oregon State University. Samples were pre-treated with the bleach method using sodium hypochlorite adjusted to pH 9.5 to remove organic matter and air-dried (Mikutta et al., 2005; Soil Survey Staff, 2014). The dried samples remained in a desiccator prior to analysis. Briefly, 20 g of mineral soil was dispersed with 5% sodium hexametaphosphate and shaken for 10 h (Gee & Bauder, 1986). Silt and clay fractions were characterized as coarse silt (20–50 μm), fine silt (2–20 μm), and clay (<2 μm). The sand fraction was wet-sieved into five fractions: very coarse sand (1000–2000 μm), coarse sand (500–1000 μm), medium sand (250–500 μm), fine sand (100–250 μm), and very fine sand (50–100 μm).

2.5 | Soil development indices

The PDI was calculated for every soil profile in the study using rubification, melanization, consistence, structure, stickiness, plasticity, and texture (Harden, 1982; Harden & Taylor, 1983). The PDI values are based on assigned points for soil development compared to the parent material for each lithology. Increasing values for each of the properties indicates a greater degree of soil development (Harden, 1982; Harden & Taylor, 1983).

The POD Index was also determined for all profiles that contained an E horizon above B horizons (Schaetzl & Mokma, 1988). The POD Index was calculated using the difference in Munsell values between the E horizon and the uppermost B horizon and quantifying the number of Munsell hue page changes between the two horizons (Schaetzl & Mokma, 1988). Six soil profiles were not included in the POD Index calculations due to the profile either missing an E horizon or containing a B horizon Munsell color value that was greater than the overlying E value.

2.6 | Statistical analysis

All statistical analyses were performed using R version 4.0.3 (R Core Team, 2020). Simple linear regressions were used to test for relationships between carbon and clay content across lithologies. One-way analyses of variance were used to test for significant differences among soil properties (SOC stocks, bulk density, pH, depth-weighted PSA, and PDI) with respect to lithology and aspect. Depth-weighted averages were calculated for bulk density, pH, and PSA. For depth-weighted pH, if the lowermost horizon in a soil profile did not have a defined depth, that horizon was not included. SOC distribution data were visualized as a function of both average SOC

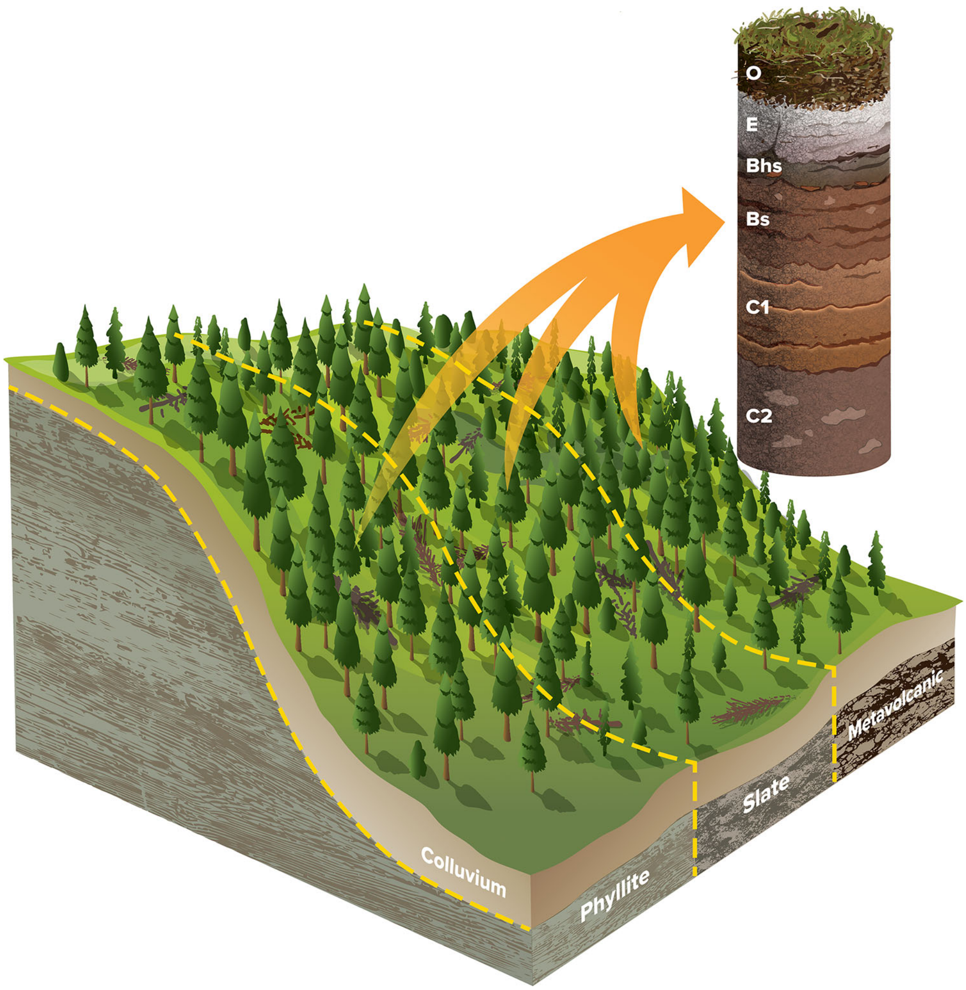

FIGURE 3 Overview illustration demonstrating the consistency in soil morphological observations recorded for upland soils in coastal temperate rainforest near Juneau, Alaska. The detailed morphological observations and horizon designations for each soil are available in Table A2. Illustration created by Rob Riedel, UC Davis IET Academic Technology Services.

stocks observed among contrasting morphological soil horizons (i.e., O, E, and B horizons) in addition to depth increment categories that represented surface (0–30 cm) and subsurface soil depths (30–50 cm; 50–100 cm). Residuals from the fitted models were checked graphically and found to reasonably meet the assumptions of constant variance and normality.

3 | RESULTS

3.1 | Soil morphology, development, and taxonomic classification

Moderately deep, acidic, very gravelly mineral soils consistently developed on steep backslopes throughout our study sites regardless of lithology or aspect (Figure 2; Figures A2–A7; Tables A2–A10). The soils are mature, well-developed Spodosols that presented few distinctions in soil properties (Figure 3). Mean soil pH ranged from 3.88 ± 0.09 to 4.12 ± 0.26 in organic horizons versus 4.81 ± 0.43 to 4.94 ± 0.37 in mineral horizons (Table A4). Coarse fragments were also abundant throughout all mineral soil horizons with an overall average of 52% ± 20% (Table A2). The soils derived from slate were the deepest soils on average (115 cm ± 18 cm) compared to soils formed from the phyllite (99 cm ± 36 cm) or metavolcanic lithologies (79 cm ± 48 cm; Table A2).

The soils comprised thick organic horizons (i.e., Oi, Oe) that blanketed mineral E horizons and well-expressed spodic B horizons in a common sequence of Bh-Bhs-Bs (Figure 2; Table A2). The organic horizons formed as slightly to moderately decomposed Oi and Oe horizons, with a mean thickness of 8 ± 3 cm and 6 ± 2 cm, respectively (Table A2). Thin, wavy, and discontinuous E horizons formed beneath the organic horizons in all but three soil profiles where E horizons were absent (Table A2). Mineral “A” horizons were not observed in any of the soils we described (Table A2). The most prominent evidence for soil development occurred as dark to redder hues and subangular blocky structural development in spodic

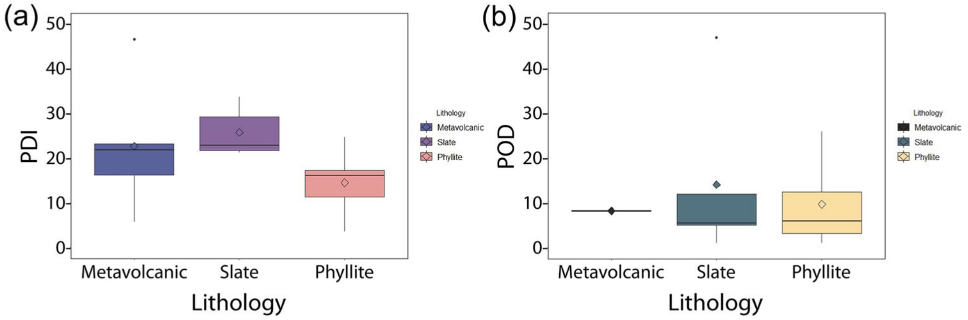

FIGURE 4 Box plots of Profile Development Index (PDI) and Podzolization Index (POD) values calculated for soils developed on contrasting lithology types in the perhumid coastal temperate rainforest of southeast Alaska. (a) PDI values and (b) POD values calculated for each soil profile as a function of lithology. *Note*: POD values were not calculated for Spodosols that contained no E horizon or a Bh, Bhs, or Bs horizon where the Munsell color value was greater than that for the overlying E value. The diamond symbols in the figure indicate mean values, and the vertical lines represent standard deviation (SD).

B horizons, with a mean thickness of 23 cm ± 19 cm. The Bh, Bhs, and Bs horizons presented mean thicknesses of 6 cm ± 2 cm, 10 cm ± 4 cm, and 25 cm ± 17 cm, respectively (Table A2). The accumulation of organic carbon in the Bh and Bhs horizons contributed to blacker soil colors (10YR 2/1 or 7.5YR 2.5/1) compared to Bs horizons with redder hues (7.5YR 2.5/2, 5YR 3/3, or 2.5YR 4/3; Figure 2; Table A2). C horizon colors varied from yellow (i.e., 2.5Y) to yellow-red hues (i.e., 7.5YR and 10YR). Values and chroma ranged from lighter (i.e., 4/2) to darker (i.e., 3/2) as imparted by parent material type (Table A2).

The majority of soil profiles sampled met the diagnostic criteria for Spodosols with little to no variation in taxonomic classification by lithology or aspect (Table A2). Haplocryods and Humicryods were found across all lithologies with more than 50% of the soils classified as Humicryods due to >6% SOC in 10 cm or more in the spodic horizons. Several south-facing soils were classified with lithic subgroups due to slightly shallower soil profiles with depths to <50 cm. Nearly half of the profiles met the requirements for andic criteria pertaining to low bulk mineral densities (mean range of 0.35 ± 0.07–0.45 ± 0.16 g cm^{-3}; Table A2) and amorphous extractable Al and Fe contents (Spinola et al., 2022). We did note that a greater proportion of soils with the andic subgroup classification occurred in the metavolcanic and slate lithologies (43% each) versus phyllite (14%).

The degree of soil development did not significantly vary by lithology or aspect as assessed by the PDI and the POD Index (Figures 3 and 4; Table A10). The slate soils presented an average PDI of 26 ± 5.27 compared to 22.70 ± 15 for metavolcanic soils, and 14.50 ± 6.62 for soils derived from phyllite (Figure 4a; Table 1). The variation in PDI was primarily driven by melanization, a proxy for soil darkening as well as rubification, or the reddening of the soil. Both melanization and rubification significantly varied with lithology (Table 1). Rubification differed by lithology with the highest values in soils formed from the metavolcanic rock (0.50 ± 0.13) versus those from slate (0.44 ± 0.04) and phyllite (0.35 ± 0.11) (Table 1). Slate soils presented the highest melanization score (0.15 ± 0.05) compared to metavolcanic (0.09 ± 0.09) and phyllite soils (0.02 ± 0.06; Table 1). The values for the POD Index were also consistent where the highest POD Index value of 14.10 ± 18.80 coincided with the slate lithology (14.10 ± 18.80) compared to 9.75 ± 11.20 for phyllite, and 8.25 ± 0.35 for the metavolcanic soils (Table 1; Figure 4b).

The most common textures in all soils were sandy loam, loam, and silt loam (Figure 5) where total sand, silt, and clay were relatively consistent across lithologies (Table A5; Figure A8). The slight variations in texture were driven mostly by differences between the sand and silt fractions (Table A5; Table A6). We did observe significant differences when comparing the distribution of coarse to fine sand fractions (Table A6). Soils formed from the metavolcanic lithology contained significantly more very fine sand (8.03% ± 2.22%) than those from the slate (4.28% ± 0.74%) and phyllite (5.94% ± 1.21%) lithologies.

3.2 | Distribution of SOC

The distribution of SOC stocks across organic and mineral horizons is consistent among all sites regardless of lithology or aspect (Table A7). We found an appreciable higher proportion of SOC in mineral horizons (71%) rather than the organic horizons (29%; Figure 6a; Table A7). We compared the distribution of SOC by morphological horizon across all soil profiles (cumulative O, E, and B horizons) and found that cumulative O horizons contained SOC stocks ranging from 51.76 ± 18.11 Mg C ha^{-1} to 69.94 ± 39.76 Mg C ha^{-1} (Figure 6a; Table A7). We measured lower SOC stocks in the E horizons spanning 3.79 ± 6.57 Mg C ha^{-1} to 16.77 ± 3.98 Mg C ha^{-1} (Figure 6a; Table A7). The thick B horizons contained the highest SOC stocks with average values ranging from 91.15 ± 89.89 Mg C ha^{-1} to 157.15 ± 128.20 Mg C ha^{-1}

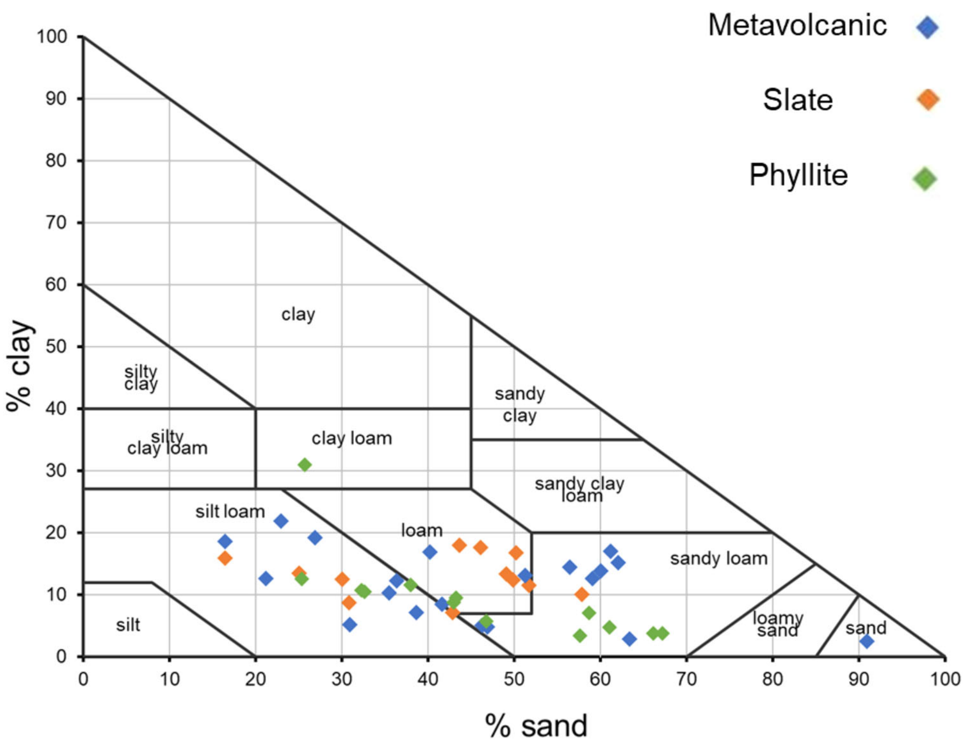

FIGURE 5 A textural triangle depicting clay and sand percentages for each soil profile sampled in upland landscapes of the perhumid coastal temperate rainforest near Juneau, Alaska. Each color represents a distinct lithology as indicated in the legend.

FIGURE 6 Stacked bar graphs showing the distribution of soil organic carbon (SOC) in each lithology type by morphological horizon and depth. (a) Average soil organic carbon stocks for summed organic and mineral horizons and (b) absolute soil organic carbon stocks by depth intervals of 0–30 cm in dark blue, 30–50 cm in pink, and 50–100 cm in yellow. The standard deviations associated with the SOC data presented in Figure 6 are available in Table A8. SOC is abbreviated as carbon in the figure.

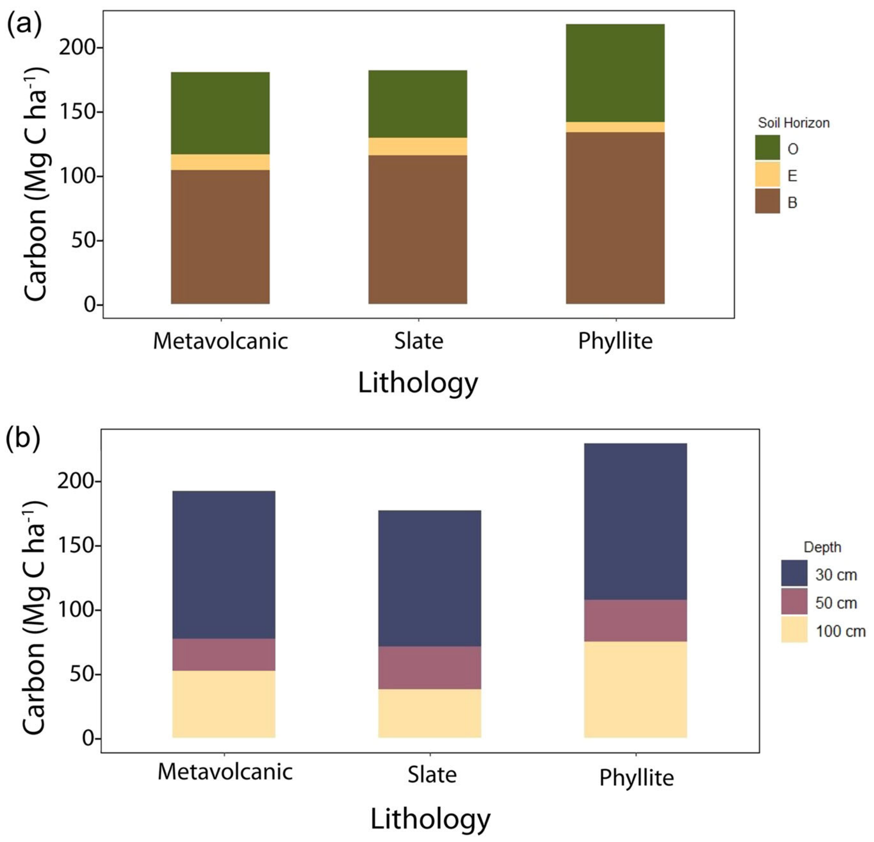

TABLE 1 One-way analysis of variance (ANOVA) results using lithology as the main effect for the Podzolization Index (POD), Profile Development Index (PDI), rubification, melanization, structure, and texture of soil profiles found in the perhumid coastal temperate rainforest of southeast Alaska.

Lithology	POD	PDI	Rubification	Melanization	Structure	Texture
Metavolcanic	8.25 ± 0.35 A	22.70 ± 15.00 A	0.50 ± 0.13 A	0.09 ± 0.09 A	0.39 ± 0.04 A	0.29 ± 0.11 A
Slate	14.10 ± 18.80 A	25.80 ± 5.51 A	0.47 ± 0.07 B	0.16 ± 0.06 B	0.37 ± 0.10 A	0.20 ± 0.11 A
Phyllite	9.75 ± 11.20 A	14.20 ± 6.62 A	0.35 ± 0.11 C	0.02 ± 0.06 C	0.37 ± 0.04 A	0.30 ± 0.17 A

Note: Means with the same letter in each lithology are not significantly different ($p < 0.05$). For the POD Index, we did not use six profiles (P5, P7, P10, P11, P15, and P17) due to either a missing E horizon or a B Munsell color value that was greater than the overlying E value. For the PDI, we did not use P10 due to the presence of only one mineral horizon and the classification as a Histosol. Using lithology as the main effect for the POD Index: Metavolcanic $n = 2$, slate $n = 5$, and phyllite $n = 4$. Using lithology as the main effect: Metavolcanic $n = 5$, slate $n = 5$, and phyllite $n = 7$.

(Figure 6a; Table A7). The B horizons of the phyllite soils contained slightly higher SOC stocks (146.15 ± 91.85 Mg C ha^{-1}) compared to metavolcanic (118.21 ± 75.05 Mg C ha^{-1}) and slate soils (120.29 ± 13.84 Mg C ha^{-1}), albeit insignificant (Table A7). The distribution of SOC was variable where the coefficient of variance (CV) fluctuated greatly for the B horizons including CVs of 62.84% for phyllite, 63.49% for metavolcanic, and 11.50% for slate soils (Table A7).

We also compared total SOC distribution by discrete depth increments to provide insight on how soil sampling at shallow depths (<30 cm) would impact carbon stock budget estimations in the NPCTR. Our results indicate that almost 40% of total SOC would not be accounted for if sampling had been restricted to the upper 30 cm of soil. The 0- to 30-cm depth increment integrates O, E, and upper spodic B horizons in most soil profiles (Figure 6) and included 61% of the SOC accumulated in the soil. We found that total mean SOC stocks in the 0- to 30-cm depth increment ranged from 105.57 ± 30.03 Mg C ha^{-1} to 121.79 ± 64.76 Mg C ha^{-1} and that the 30- to 50-cm depth contained mean SOC stocks of 30.05 ± 14.24 Mg C ha^{-1} to 32.02 ± 22.83 Mg C ha^{-1}. SOC distribution in the remaining 50- to 100-cm depth interval presented mean SOC stocks spanning 44.50 ± 12.56 Mg C ha^{-1} to 74.82 ± 66.23 Mg C ha^{-1} (Table A8). Therefore, when assessing SOC distribution within the upper 30 cm, it is important to note that the Bh mineral horizons contribute significantly to the overall carbon stocks (Figure 6b).

Overall, the studied soils contained abundant carbon stocks that were consistent across all lithologies on north-facing and south-facing slopes (Table A9). An overall mean pedon SOC stock of 198.02 ± 81.42 Mg C ha^{-1} was calculated using data collected for all upland organic and mineral soils analyzed in the 18 soil profiles surveyed during the project. The phyllite soils presented the largest mean carbon stock, with 218.00 ± 124.00 Mg C ha^{-1}, but this value was not statistically different than averages of 188 ± 53.80 Mg C ha^{-1} and 182 ± 15.70 Mg C ha^{-1} for the metavolcanic and slate lithologies, respectively (Table A9). Despite the phyllite soils containing slightly greater mean carbon stocks per pedon, the CV was 56.88% of the mean, whereas the CV for metavolcanic (28.62%) and slate (8.63%) lithologies were much narrower.

4 | DISCUSSION

4.1 | Soil development in upland coastal rainforest soils

4.1.1 | PDI and the POD Index

The Spodosols in our study were well-developed and shared similar soil chemical, physical, and morphological properties regardless of lithology or aspect as quantified using the PDI (~14–26) and the POD Index (~8–19; Table 1; Figures 2 and 3; Table A10). We observed relatively high PDIs in our sites given that the soils formed in mid-late Holocene landscapes versus published findings for older soils in other climates. For example, original work on the PDI calculated index values of 12–34 for soils in an aridic climate (New Mexico, USA) that were approximately 20,000 years old and index values of 5–18 for soils that were ~4000 years old (Harden & Taylor, 1983). Soils formed in a similar post-glacial setting under a Udic moisture regime had index values from 4 to 15 in soils of Holocene age (11,000 to 15,000 years) and index values of 37–39 in soils with age estimates of 40,000 years (Harden & Taylor, 1983). Therefore, the soils of southeast Alaska displayed PDIs that tend toward values of much older soils in the context of the desert and temperate studies.

Profile development indices in Arizona increased along a bioclimate sequence from ~3 to 17 with the highest value in mixed-conifer stands with soils of Holocene age (Lybrand & Rasmussen, 2015). The PDIs in Arizona corresponded to the expression of melanization, structure, and rubification in granitic soils supporting subhumid pine and mixed conifer forests in southern Arizona (Lybrand & Rasmussen, 2015). A geomorphologic investigation of glacial deposits in the Lake Tahoe Basin, California, observed PDIs of 29–45 in mixed conifer forest that increased as a function of age (Aburto &

Southard, 2017). The youngest deposits at ∼15,000 years had index values below 20, while soils that were ∼25,000 years had values from 15 to 24 (Aburto & Southard, 2017). The soils of southeast Alaska displayed PDI values that range higher as a result of forming under more intense weathering conditions with greater organic matter inputs that accelerate mineral weathering and promote soil development compared to PDIs published for soils in contrasting climates (i.e., desert southwest; subhumid Arizona forest; and mixed conifer forest near Lake Tahoe, California).

The PDI is an important tool for comparing the intensity of soil development across all soils, whereas the POD Index provides a specific comparison related to the development of spodic horizons. Spodosols form rapidly (<300 years) in southeast Alaska and are well developed (Alexander & Burt, 1996; Chandler, 1943; Crocker & Dickson, 1957). The POD Index supports this observation in a quantitative manner given that POD values spanned ∼8–14 in our field areas (Table 1; Figure 4b). The observed index values range from 0 to 72 along chronosequences, toposequences, and hydrosequences in varying climates (Arbogast & Jameson, 1998; Goldin & Edmonds, 1996; Schaetzl et al., 2006; Schaetzl & Mokma, 1988; Schaetzl & Thompson, 2015; Valerio et al., 2016; Wilson, 2001). The lowest calculated POD values spanned 0 to 0.56 for young, weakly developed Spodosols in the coastal dunes of Michigan where soil profiles included one thin E horizon underlain by a single Bs horizon (Arbogast & Jameson, 1998). POD values of 0–2 were observed in post-glacial soils that formed in a mixed conifer forest on sandy outwash parent material in Michigan; index values here were attributed to thicker organic horizons and exposure to long periods of snowmelt infiltration (Arbogast & Jameson, 1998; Schaetzl et al., 2006).

Spodosols that formed under cryic temperature regimes in Michigan presented POD values of 6–11 where soils with Humic great group classifications exhibited higher index values than those with Typic great groups (Schaetzl & Mokma, 1988; Schaetzl & Thompson, 2015). This coincides with our findings, where Humicryod great groups displayed slightly higher POD values than the Haplocryods, likely due to the expression of darker Bh horizons in the Humicryods (Table A2). Notably, a similar mean POD Index value of ∼18 was determined for 172 Spodosols (i.e., Aquods and Humods) formed under warm, wet climate conditions in Florida that included thermic and hyperthermic soil temperature regimes (Goldin & Edmonds, 1996).

Overall, the PDI and POD values in our study were relatively high when compared to published findings for soils formed on coarse-textured parent materials under temperate climates during the Holocene or earlier (Arbogast & Jameson, 1998; Birkeland, 1994; Goldin & Edmonds, 1996; Harden & Taylor, 1983; Lybrand & Rasmussen, 2015; Miller & Birkeland, 1992; Schaetzl & Mokma, 1988; Schaetzl & Thompson, 2015; Wilson, 2001). Our study highlights the critical role that bioclimatic factors (i.e., perhumid climate, cool temperature, and acidic vegetation inputs) play in driving the formation of Spodosols in southeast Alaska.

4.1.2 | Soil morphological properties

We observed a strong influence of bioclimatic factors as drivers of pedogenesis in southeast Alaska across our field areas (Alexander et al., 1993; Heilman & Gass, 1974). The combination of a wet precipitation regime (∼1600 mm mean annual precipitation [MAP], mean annual snowfall of ∼2200 mm), cool climate (mean annual temperature [MAT] 5.6˚C), and acidic vegetation (western hemlock, Sitka spruce) creates the intense weathering and leaching environment required to form well-developed soils even on steep hillslopes (Figure 2a,c,e). Moreover, the absence of fire in southeast Alaska allows live and dead biomass to accumulate above-ground, including mosses, which are known for increasing water storage, supplying organic acids, and enhancing weathering processes (Musielok et al., 2021). We suggest that interacting factors such as steep topography, a wet climate, abundant vegetation, the possible admixture of aeolian silt (i.e., Eger et al., 2012), and natural disturbance events (e.g., tree throw; Lewis, 1976; Bormann et al., 1995) may shape the rapid development of Spodosols in temperate rainforest upland landscapes.

We consistently found thick organic horizons (∼7 cm on average) over patchy and thin mineral E horizons, an absence of A horizons, and the presence of thick spodic horizons (Figure 2). Thin, patchy, and broken E horizons were observed in 70% of the 18 soil profiles (Table A2), which we attribute to disturbance including tree throw events as hypothesized for the patchy distribution or complete absence of E horizons in Spodosols on Vancouver Island (Lewis, 1976). Pedoturbation driven by tree throw mixes surficial soil horizons through the physical disruption of tree roots when trees tip or are completely uprooted (Bormann et al., 1995). Our findings also align with previous work in southeast Alaska that found A horizons to be entirely absent in soils older than 90 years and that E horizons can form in 70 years due to the intense leaching environment (Alexander & Burt, 1996). In contrast, E horizons generally develop over 170 to 1000 years in other climates of North America (Sauer et al., 2007).

The absence of A horizons in the Spodosols of southeast Alaska has been attributed to a combination of factors including the wet and cool climate, rapid soil formation rates, limited bioturbation by organisms, strong acidity, and the slow decomposition of litter. In the region, A horizons are typically only observed in very young soils (<80 years old) along regional soil chronosequences (Alexander & Burt, 1996). At this initial stage, the dominant deciduous trees contribute litter with rapid turnover, a higher N concentration, and the potential for mixing with mineral soils, which facilitates the formation of incipient A horizons. However, the A horizons quickly transform into E horizons due to the succession of coniferous vegetation, such as Sitka Spruce and Western Hemlock, which occurs around 70–100 years following glacial retreat. Western Hemlock and Sitka Spruce produce more slowly decomposing, acidic litter with a high CN ratio. Bioturbation by organisms, such as earthworms or termites, is one of the processes contributing to the formation of A horizons that is virtually absent in the Spodosols of the region. Moreover, dense carpets of moss develop within 100 years of deglaciation (Alexander & Burt, 1996). The moss carpets may accelerate weathering by contributing acidity and increasing the water-holding capacity of the soil, which ensures consistent moisture levels during brief summer dry spells while also providing enhanced thermal insulation that may allow water to remain liquid in the soil for more extended time periods during winter. These conditions are ideal for rapid E horizon formation where intense mineral weathering releases Fe and Al oxyhydroxides from silicates and subsequently forms organometallic complexes that bind and mobilize the oxyhydroxides.

The fine-grained silt loam and loam textures of the Spodosols in our study also likely contributed to the thin, patchy distribution of E horizons as noted in other Spodosol development research where soil texture played a defining role (e.g., Schaetzl & Harris, 2012; Valerio et al., 2016). Prominent E horizons were observed in coarser-grained, granodiorite and tonalite moraine soils of the Mendenhall Valley, Alaska (Alexander & Burt, 1996), and incipient E horizon development was also documented in young moraine Spodosols of Glacier Bay, Alaska (Goldthwait et al., 1966). E horizons were weakly expressed in loamy Spodosols from Michigan and New York (Schaetzl & Harris, 2012). Soil texture influenced the development of Spodosols in northern Idaho where soils with coarser textures presented thicker E horizons (14–18 cm) compared to E horizons in finer-textured soils (~5 cm; Valerio et al., 2016). The northern Idaho study also found that coarser textured Spodosols formed in volcanic ash over glacial till or sandy outwash and were associated with thicker E horizons. The thin E horizons in silt loam Spodosols formed from metasedimentary rock occurring beneath ash suggested that parent material texture inhibited morphological expression and soil development (Valerio et al., 2016).

One of the most notable morphological properties was the prominence of thick spodic B horizons (23 ± 19.32 cm) that contained complete sequences of Bh, Bhs, and Bs horizons in 72% of the described soil profiles (Table A2). The prevalence of the Bh-Bhs-Bs sequence reflects podzolization processes that result from both (i) a cool, humid climate (Lundström et al., 2000; McKeague et al., 1983; Sanborn et al., 2011; Schaetzl & Isard, 1991) and (ii) acidic inputs from organic horizons, fungi, microorganisms, and root exudates from plants (Lundström et al., 2000; Sauer et al., 2007; Schaetzl & Thompson, 2015). Very fine to coarse-sized roots were observed throughout all the profiles including the spodic B horizons and often the B/C combination horizons (Table A2). The spodic horizons may have formed from the illuviation of organometallic complexes transported into the mineral soils from the overlying organic horizons (Buurman & Jongmans, 2005; Sauer et al., 2007) or from root-derived acidic inputs to the subsurface horizons (Billings et al., 2018; Harper & Tibbett, 2013; Sauer et al., 2007).

Our observations align well with work conducted in the Black Forest, Germany, where Bh-Bhs-Bs horizon sequences formed on steep hillslopes in periglacial slope deposits under cold, wet conditions that promoted intensive leaching (6.5°C MAT, 1300 mm MAP; Sauer et al., 2007). Likewise, the wet maritime climate of coastal British Columbia, Canada, influenced the development of organic-rich Bh horizons above the sesquioxide-enriched horizons in humic Podzols (Sanborn et al., 2011). Complete spodic horizon sequences were also described for Spodosols in New Hampshire that formed under similar bioclimatic conditions with slightly less precipitation and more acidic parent material (i.e., 1400 mm MAP; Bourgault et al., 2015; Ussiri & Johnson, 2004). Interestingly, the work suggested that lateral podzolization may explain the occurrence of Bh and Bhs horizons in soils found on lower backslopes and bench positions given that transported water contained amorphous organometallic complexes from upslope Spodosols (Bourgault et al., 2015; Ussiri & Johnson, 2004). Prior work also found that topography influenced the formation of Spodosols on flysch-derived hillslopes in the Outer Western Carpathians of southern Poland where Spodosols formed in the middle slope positions compared to an absence of podzolization in hillslope positions experiencing active geomorphic processes and the deposition of aeolian silts (Musielok et al., 2022). We hypothesize that the steep backslopes encouraged lateral water flow downslope in our field areas, which suggests the potential importance of lateral podzolization in these upland ecosystems. Since our work focused specifically on soils in backslope positions, future investigations would need to include a catena sampling design to address the hypothesis that lateral podzolization serves as a soil formation mechanism across the upland hillslopes.

4.1.3 | Expression of andic properties

Greater than 50% of sampled profiles were classified with an andic subgroup designation including those with lithologies of no volcanic origin (Table A2). The soils that met the requirements for the andic subgroup classification displayed high organic carbon percentages (up to 19% SOC in mineral soil horizons), low bulk density values (<0.9 g cm^{-3}), and concentrations of oxalate extractable Al+$^{1/2}$Fe > 2% (Spinola et al., 2022). We did note that soils derived from the phyllite lithology had a much lower proportion of soils containing the andic subgroup classification at 14% versus 43% for both the metavolcanic and slate soils (Table A3). We attributed this to shallower depth to parent material or transitional BC horizons (Figures A2–A4) and a lower degree of melanization or soil darkening in the phyllite soils (Table 1). Overall, the expression of andic properties in non-volcanic soils results from the combination of a cool, wet climate, which promotes rapid weathering and leaching, the integration of organics with mineral particles, and the accumulation of Fe and Al oxides in subsurface horizons.

Our findings align with previous work conducted in southeast Alaska which reported that nearly two-thirds of spodic horizons display andic properties in volcanic and non-volcanic lithologies, such as granite, phyllite, schist, mixed alluvium, limestone, and mixed colluvium over till (Alexander et al., 1993; Farr & Ford, 1988). Andic soils are known to contain large amounts of SOC in combination with exhibiting high water retention capacity and unique soil properties that positively influence soil fertility (Iamarino & Terribile, 2008) while also promoting the accumulation and persistence of SOC in both volcanic and non-volcanic soils (Matus et al., 2014; Terribile et al., 2018). Andic properties in non-volcanic parent material are not widely common yet do occur across a range of parent materials (e.g., Bäumler et al., 2005) and in similar temperate climates throughout the world (e.g., Garcia-Rodeja et al., 1987; Mileti et al., 2017). Andic properties were found in a series of well-drained soils formed in basic parent materials (i.e., amphibolites and schists) on slopes with heath vegetation in cool, humid climates of Spain (MAP 1010–1860 mm; MAT 12–14˚C; Garcia-Rodeja et al., 1987). Andic properties were also noted in soils derived from fine silt loess on steep slopes (15–60%) under cool and humid climate conditions in Italy that enabled the accumulation of organic matter, loess weathering, and the enrichment of organo-metallic complexes (Mileti et al., 2017). Research in the Italian Non-Volcanic Mountain Ecosystems (NVME) emphasized the need for andic soils to be more clearly recognized in soil classification given their ecological and agricultural importance and that andic soils have been underestimated, especially in mountain ecosystems, both in the Italian NVMEs and likely elsewhere (Iamarino & Terribile, 2008).

4.1.4 | Influence of soil texture on the development of Spodosols

Spodosols formed under temperate climates tend toward coarser textures that facilitate the eluvial/illuvial process of podzolization (Schaeztl & Harris, 2012). Conversely, the textures for the majority of the soil profiles we sampled comprised finer textures of silt loam, loam, and sandy loam (Figure 5). We also noted that the textures of the soils derived from slate comprised almost exclusively silt loam and loam textures, with the exception of one observation, whereas the phyllite and metavolcanic soils spanned sandy loam, loam, and silt loam textural classes. We predict that the finer grained soil textures in the slate soils were likely imparted by the very fine-grained textures of slate bedrock compared to fine-grained phyllite and metavolcanic rock. While we did not observe significantly higher PDI or POD values for slate soils in our study, we did note that the PDI and POD Index values for slate soils were higher than those calculated for the phyllite and metavolcanic soils. We observed significantly higher melanization scores in the slate soils versus the other two rock types and a significantly higher rubification score in slate soils when compared to phyllite soils (Table 1). Prior work also found slate soils to exhibit the highest weathering index values for Spodosols, the greatest depletion in base cations, and the largest concentration of Fe oxides at depth when compared to phyllite, tonalite, and metavolcanic soils (Spinola et al., 2022). The greatest degree of soil development does appear to correspond to slate soils with finer textural classes (Figures 4 and 5; Table 1; Spinola et al., 2022); however, more work is required to decipher the intricate mechanisms that may be driving these differences.

The soil matrix for each profile also contained an abundance of rock fragments from 1.5% up to 89.7% (Table A2), which likely influenced soil development processes by promoting the preferential flow of water and the translocation of Fe- and Al-oxides and organics to deeper horizons (Schaetzl, 1991a; Schaetzl & Thompson, 2015). The soils of southeast Alaska form thick, diverse spodic horizons compared to Spodosols in Michigan where acidic, coarse-textured parent materials with >82% rock fragments contributed to less total surface area, low water-holding capacity, and a limited amount of chemically reactive surface sites (Schaetzl, 1991b). While the soils we studied contain, on average, fewer coarse fragments than the study in Michigan (51.8 ± 20.4%; Table A2), the abundant rock fragments likely increased drainage and contributed to soil formation. Moreover, no redoximorphic features were observed in the described soils despite finer grained textural classes and the perudic soil moisture regime (Table A2). The steep backslope landscape position along with the abundant rock fragments promoted soil development through the transport of water, organics, and other soluble weathering products both vertically in the soil profiles and laterally downslope (Figure 2; Table A2).

4.2 | Accumulation of SOC in the NPCTR

Our assessment of SOC distribution in 18 soil profiles quantified soil organic carbon stocks in colluvium-derived mineral soils common to the post-glacial landscapes of the Northeast Pacific Coastal Temperate Rainforest. The intensive survey of upland soil profiles revealed several important findings. First, the mean pedon SOC stock calculated across all sites was 198.02 ± 81.42 (n = 18), which was slightly lower than the average of 228 ± 111 Mg C ha^{-1} calculated from models of carbon stocks as determined from a regional soil database that included all soil types across the NPCTR (McNicol et al., 2019). This observation is especially notable and demonstrates the impact of carbon-rich mineral soils in this region given that McNicol et al.'s (2019) study included organic soils with averages of 800–1000 Mg C ha^{-1} in the overall calculation. The resolution gained by focusing on specific positions on the landscape (i.e., backslopes) and soil types (i.e., Spodosols) provided a more constrained estimate of SOC in upland soil units than from regional models. Second, lithology and aspect did not appear to exert strong control on SOC stocks given that we noted the consistent accumulation of SOC on steep backslopes in soils formed from contrasting lithologies on north- and south-facing slopes. We recognize that topography and relief-induced microclimates influence the spatial heterogeneity of SOC across ecosystems (e.g., Macyk et al., 1978; Patton et al., 2019; Zhu et al., 2019). However, bioclimatic factors (i.e., perhumid climate, cool temperature, and acidic vegetation) appeared to play the most prominent role in the relatively consistent and similar distribution of SOC in the studied Spodosols of the NPCTR. Further, SOC accumulated to the greatest degree in the spodic horizons compared to the overlying organic horizons (Figure 6a); this finding has important implications for SOC persistence given that the formation of organometallic complexes in subsurface soils has been found to influence and increase the persistence of SOC (Kleber et al., 2005; Kögel-Knabner et al., 2008; Schulze et al., 2009; Rumpel & Kögel-Knabner, 2011).

4.2.1 | SOC depth distribution

We observed that 70% of total SOC stocks occurred in the spodic horizons, similar to global estimates of up to 66% of total pedon SOC distributed in spodic horizons (Johnson et al., 2011; Kögel-Knabner & Amelung, 2021; Stone et al., 1993). The largest quantities of SOC accumulated as moderately deep carbon (>30 cm deep) in thick spodic B horizons (118.21 ± 75.05 Mg C ha^{-1} to 146.15 ± 91.85 Mg C ha^{-1}; Figure 6; Table A7). We found that the Bh and Bhs horizons contained the greatest proportion of SOC in the subsurface horizons (range of 3%–19% C; Table A3) with SOC percentages slightly higher compared to other temperate climates of the world such as Germany (1.8%–4.8% SOC, Sauer et al., 2007), southern Poland (6.16%–12.6% SOC, Musielok et al., 2021), northern Idaho (1.4%–7.8% SOC, Valerio et al., 2016), and Denmark (2.41%–4.15% SOC; Verje et al., 2003).

Our findings were consistent with the range of SOC percentages in spodic horizons of southeast Alaskan Spodosols formed in similar parent materials on backslope positions (25%–35% slope) in Holocene deposits (3.62%–12.02% SOC, D'Amore et al., 2015) and on a 14% slope dominated by slate and phyllite (13.7%–18.3% SOC, Alexander et al., 1993). The deep carbon results from podzolization processes that include the downward transport and accumulation of SOC in spodic horizons as a result of acidic vegetation biomass inputs, the persistent delivery of precipitation, and cool temperatures. It is also possible that the steep slopes found in our field areas drive the lateral transfer of SOC-rich solutes and water that may promote lateral podzolization (Sommer et al., 2001; Gannon et al., 2014).

Soil organic carbon content more than doubled with depth in forest soils of the Pacific Northwest (Homann et al., 2004; James et al., 2014; Smithwick et al., 2002), which supports our finding that large quantities of SOC accumulate in subsurface B horizons (Figure 6). Assessments of Pacific Northwest old-growth forest soils found that mean SOC stocks doubled from 58 ± 29 Mg C ha^{-1} in the first 20 cm to 133 ± 87 Mg C ha^{-1} in the upper 100 cm (Homann et al., 2004). A systematic study on deep carbon in a coastal Pacific Northwest forest found that sampling to 2.5-m depth (versus 0.5 m) increased total SOC stocks by 156% (James et al., 2014). Interestingly, SOC increased from 20.9 Mg C ha^{-1} at 1 m to 47.5 Mg C ha^{-1} at 2.5 m across a wide variety of parent material that included volcanic ash, sedimentary derived colluvium, residuum, till, volcanic rock, and lacustrine deposits in temperate rainforests (James et al., 2014). More work focused in the Oregon and Washington coastal temperate rainforests found SOC stocks varied from 109 to 472 Mg C ha^{-1} when measured up to 1-m depth where minimal fire and little storm disturbance promoted the accumulation of carbon in the soils and standing large trees (Smithwick et al., 2002).

4.2.2 | Pedon SOC stock accumulation in upland soils

We found large, similar quantities of SOC stocks for all upland organic and mineral soils from our work, with an overall mean pedon SOC stock of 198.02 ± 81.42 Mg C ha^{-1} (n = 18). Our data sets support prior findings indicating that temperate rainforests serve as one of the leading bioregions for SOC abundance in the world. SOC values in the present study were comparable to a median of 211 Mg C ha^{-1} found in coastal temperate forests from northern California to southeast Alaska (Carpenter et al., 2014), and a mean of 179.1 Mg C ha^{-1} in the temperate forested region of northeastern China (Wei et al., 2013). In a study of Oregon and Washington coastal forests, mean SOC was 286 ± 103 Mg C ha^{-1} with the Oregon coast accumulating substantially higher SOC in cool, wet climates that promoted vegetation growth in the absence of forest fire disturbance (Smithwick et al., 2002). Overall, lithology and aspect did not exhibit significant control over the accumulation of SOC in our study (Figure 6; Table A9), likely due to the overpowering influence of a wet, cool climate coupled with an abundance of organic inputs from the forested ecosystem.

Prior work in the Pacific Northwest and Alaska found few associations between lithology and topography on SOC distribution (Alexander et al., 1993; Heilman & Gass, 1974). According to estimations of data gathered from dominant soil series found in the NRCS database (Soil Survey Staff, 2013), the median SOC in the North Pacific Coastal Temperate Rainforest (northern California to southeast Alaska) is 211 Mg C ha^{-1} (range of 116–439 Mg C ha^{-1}; Carpenter et al., 2014). This estimate encompasses a broad group of soils formed from a variety of parent materials (i.e., residuum, colluvium, marine deposits, alluvium, till, and volcanic ash) and a variety of topographic factors with slopes ranging from 0% to 90% where soils depths varied (shallow to moderately deep to deep). Climate, disturbance history, topography, decomposition rates, soil development, quantity and type of organic matter, and vegetation dynamics were all identified as the dominant controls on SOC storage in temperate rainforests (Carpenter et al., 2014). Western hemlock-dominated forests were a driving factor for greater SOC stocks than Douglas-fir forests of the Puget Sound, Coastal Washington and Oregon, and Washington and Oregon Cascades (SOC ranged from 102 to 309 Mg C ha^{-1}; Edmonds & Chappell, 1994).

Soil nutrient and SOC concentrations did not vary significantly among seven Spodosols formed from different lithologies in southeast Alaska with average C percentages of 4.37% C in phyllite, 3.20% C in granodiorite, 4% C in basalt, 7.4% C in limestone, 8.38% C in volcanic ash, and 1.73% C in gravelly till (range of 1.2%–11.6% C; Heilman & Gass, 1974). Our interpretations align with those presented by Heilman and Gass (1974), who hypothesized that similar climate and vegetation inputs in southeast Alaska promoted a homogenization of soil properties in addition to SOC and nutrient cycling trends.

The relative importance of lithologic controls on SOC abundance varies by bioclimatic region, soil physical and chemical properties, and lithology type, among other factors (Alexander et al., 1993; Araujo et al., 2017; Carpenter et al., 2014; Heilman & Gass, 1974). Lithology exhibited significant control on SOC abundance across a climosequence in northeast Brazil, where clay- and iron-rich soils formed from rocks with a mafic assemblage that contained significantly higher SOC (207.6 Mg C ha^{-1}) than coarser grained soils derived from a sedimentary lithology (150 Mg C ha^{-1}; Silva et al., 2016). SOC abundance was also highest in limestone-derived soils compared to soils formed in weakly metamorphosed, calcareous and non-calcareous sedimentary rock (Catoni et al., 2016). Soils formed in temperate ecosystems in the Oregon/Washington Cascade Mountains and coasts as well as the Vancouver Island regions had significantly higher mean SOC stocks in the sedimentary-derived soils (196 ± 14 Mg C ha^{-1}) compared to soils formed from glacial (125 ± 16 Mg C ha^{-1}) and igneous parent materials (Littke et al., 2011). This was due to variances in soil nutrient regimes (based on soil depth, texture, wetness, color, and forest floor type) where soils with richer nutrient regimes had greater carbon values (137 ± 14 Mg C ha^{-1}). Lithology acted as an indirect control on SOC abundance in southern Arizona where SOC stocks in soils formed from basic limestone (35 ± 0.1 Mg C ha^{-1}) and basalt (87 ± 0.1 Mg C ha^{-1}) were significantly different from soils formed in acidic rhyolite (110 ± 0.0 Mg C ha^{-1}) and granite (53 ± 0.1 Mg C ha^{-1}; Heckman et al., 2009). The differences in SOC abundance were attributed to contrasting values in soil pH and associated SOC stabilization mechanisms (e.g., metal-humus complexation for acidic soils and mineral adsorption for basic soils). We observed mean pH values of ∼4.8–4.9 across all mineral soils derived from very fine-grained to fine-grained parent materials (Table 1), which likely contributed to similar SOC stocks and possibly to similarities in SOC stabilization mechanisms (Silva et al., 2016; Slessarev et al., 2016).

5 | CONCLUSIONS

Forest soil organic carbon accounting is an ongoing topic of research, policy discussions, and strategic development given the urgency to mitigate climate change on Earth, specifically the need to reduce greenhouse gas emissions to the atmosphere. However, SOC remains one of the most poorly constrained components of the terrestrial C cycle, especially in remote forested regions where data sets and replication by geomorphic setting are limited. Coastal temperate rainforest ecosystems present the important opportunity to address whether the degree of soil development influences soil carbon distribution under wet, cool, and productive conditions that intensify mineral weathering and promote soil formation.

Our work assessed soil morphological development and SOC distribution across 18 soil profiles in remote, upland regions of the coastal temperate rainforest near Juneau, Alaska. We found that Spodosols undergo a similar degree of soil development and accumulate SOC consistently across upland landscapes when compared across contrasting lithologies (slate, phyllite, and metavolcanic) and aspect (north and south-facing backslopes). Our findings indicate that bioclimatic factors likely have a greater impact on soil formation and SOC distribution compared to other factors, namely lithology or aspect. Over 70% of SOC accumulated in subsurface mineral horizons compared to surficial organic horizons. Specifically, we found >100 Mg C ha^{-1} distributed to mineral soils versus <50 Mg C ha^{-1} in the overlying organic horizons. Furthermore, our results indicate that almost 40% of the total SOC measured would not be accounted for if sampling had been restricted to the upper 30 cm of soil. Mineral soils with the greatest abundance of carbon coincided with sequences of well-expressed Bh, Bhs, and Bs horizons formed on upland backslopes. Podzolization represents a critical soil forming process in the soil profiles studied that likely led to the large accumulation of SOC in the subsurface. Overall, the PDI and POD values in our study were also relatively high when compared to published findings for soils formed on coarse-textured parent materials under temperate climates during the Holocene or earlier. This work established a research sampling framework for upland soils and data sets for soil formation and SOC distribution in remote, data-limited forest soils, which is especially relevant given the importance of the region to global carbon dynamics, nutrient cycling, and ultimately climate change.

AUTHOR CONTRIBUTIONS

Jennifer Fedenko: Conceptualization; data curation; formal analysis; funding acquisition; investigation; methodology; project administration; visualization; writing—original draft; writing—review and editing. **David D'Amore**: Conceptualization; data curation; formal analysis; funding acquisition; investigation; methodology; project administration; resources; supervision; visualization; writing—review and editing. **Diogo Spinola**: Conceptualization; investigation; project administration; visualization; writing—review and editing. **Raquel Portes**: Conceptualization; investigation; visualization; writing—review and editing. **Ashlee Laura Denton Dere**: Conceptualization; visualization; writing—review and editing. **Rebecca Lybrand**: Conceptualization; data curation; formal analysis; funding acquisition; investigation; methodology; project administration; resources; supervision; visualization; writing—review and editing.

ACKNOWLEDGMENTS

This work was supported by a US Forest Service Cooperative Agreement to Rebecca A. Lybrand and David D'Amore. This work was partially supported by NSF Grant CAREER EAR-2131432 to Rebecca A. Lybrand and a Geological Society of America Graduate Student Research Award to Jennifer Fedenko. The NSF CZO SAVI program also provided partial research support to Jennifer Fedenko. The authors thank Frances Biles at the USFS Pacific Northwest Forestry Station for map production and Holly Golightly, Quinn Lively, Randy Hesser, and Benjamin Pierce for laboratory and field assistance.

CONFLICT OF INTEREST STATEMENT

The authors declare no conflicts of interests.

ORCID

David D'Amore https://orcid.org/0000-0002-5481-8428
Raquel Portes https://orcid.org/0000-0003-2673-4232
Rebecca A. Lybrand https://orcid.org/0000-0001-7811-9093

REFERENCES

Aburto, F., & Southard, R. (2017). Refined geomorphologic interpretation of glacial deposits using combined soil development indices and LiDAR terrain analysis. *Soil Science Society of America Journal*, *81*, 109–123. https://doi.org/10.2136/sssaj2016.07.0211

Alaska Climate Research Center (ACRC). (2020). *Data*. https://akclimate.org/data/

Alexander, E. B. (1990, June 17–22). *Soil inventory and management in the Alaska Region* [Conference presentation]. Western Regional Cooperative Soil Survey Conference, Fairbanks, AK, United States.

Alexander, E. B., & Burt, R. (1996). Soil development on moraines of Mendenhall Glacier, southeast Alaska. 1. The moraines and soil morphology. *Geoderma*, *72*, 1–17. https://doi.org/10.1016/0016-7061(96)00021-3

Alexander, E. B., Kissinger, E., Huecker, R. H., & Cullen, P. (1989). Soils of southeast Alaska as sinks for organic carbon fixed from atmorpheric carbon-dioxide. In E. B. Alexander (Ed.), *Proceedings of watershed '89: A conference on the stewardship of soil, air, and water resources* (pp. 203–210). USDA Forest Service.

Alexander, E. B., Shoji, S., & West, R. (1993). Andic soil properties of Spodosols in nonvolcanic materials of southeast Alaska. *Soil Science Society of America Journal*, *57*, 472–475. https://doi.org/10.2136/sssaj1993.03615995005700020029x

Araujo, M. A., Zinn, Y. L., & Lal, R. (2017). Soil parent material, texture and oxide contents have little effect on soil organic carbon retention in tropical highlands. *Geoderma*, *300*, 1–15. https://doi.org/10.1016/j.geoderma.2017.04.006

Arbogast, A. F., & Jameson, T. P. (1998). Age estimates of inland dunes in east-central lower Michigan using soils data. *Physical Geography*, *19*, 485–501. https://doi.org/10.1080/02723646.1998.10642663

Baichtal, J. F., Lesnek, A. J., Carlson, R. J., Schmuck, N. S., Smith, J. L., Landwehr, D. J., & Briner, J. P. (2021). Late Pleistocene and early Holocene sea-level history and glacial retreat interpreted from shell-bearing marine deposits of southeastern Alaska, USA. *Geosphere*, *17*, 1590–1615. https://doi.org/10.1130/GES02359.1

Bäumler, R., Caspari, T., Totsche, K. U., Dorji, T., Norbu, C., & Baillie, I. C. (2005). Andic properties in soils developed from nonvolcanic materials in Central Bhutan. *Journal of Plant Nutrition and Soil Science*, *168*, 703–713. https://doi.org/10.1002/jpln.200521793

Berg, H. C., Jones, D. L., & Richter, D. H. (1972). Gravina-Nutzotin Belt; tectonic significance of an upper Mesozoic sedimentary and volcanic sequence in southern and southeastern Alaska. In *Geological survey research 1972: Chapter D* (Geological Survey Professional Paper 800-D, pp. D1–D24). United States Department of the Interior. https://pubs.usgs.gov/pp/0800d/report.pdf

Billings, S. A., Hirmas, D., Sullivan, P. L., Lehmeier, C. A., Bagchi, S., Min, K., & Brecheisen, Z. (2018). Loss of deep roots limits biogenic agents of soil development that are only partially restored by decades of forest regeneration. *Elementa: Science of the Anthropocene*, *6*, 2–19. 0.1525/elementa.287.

Birkeland, P. W. (1994). Variation in soil-catena characteristics of moraines with time and climate, South Island, New Zealand. *Quaternary Research*, *42*, 49–59. https://doi.org/10.1006/qres.1994.1053

Blackford, C., Heung, B., Baldwin, K., Fleming, R. L., Hazlett, P. W., Morris, D. M., Uhlig, P. W. C., & Webster, K. L. (2020). Digital soil mapping workflow for forest resource applications: A case study in the Hearst Forest, Ontario. *Canadian Journal of Forest Research*, *51*, 59–77. https://doi.org/10.1139/cjfr-2020-0066

Bliss, N. B., & Maursetter, J. (2010). Soil organic carbon stocks in Alaska estimated with spatial and pedon data. *Soil Science Society of America Journal*, *74*, 565–579. https://doi.org/10.2136/sssaj2008.0404

Bloom, A. A., Exbrayat, J.-F., Van Der Velde, I. R., Feng, L., & Williams, M. (2016). The decadal state of the terrestrial carbon cycle: Global retrievals of terrestrial carbon allocation, pools, and residence times. *PNAS*, *113*, 1285–1290. https://doi.org/10.1073/pnas.1515160113

Bormann, B. T., Spaltenstein, H., Mcclellan, M. H., Ugolini, F. C., Jr, K. C., & Nay, S. M. (1995). Rapid soil development after windthrow disturbance in pristine forests. *Journal of Ecology*, *83*, 747–757. https://doi.org/10.2307/2261411

Bourgault, R. R., Ross, D. S., & Bailey, S. W. (2015). Chemical and morphological distinctions between vertical and lateral Podzolization at Hubbard Brook. *Soil Science Society of America Journal*, *79*, 428–439. https://doi.org/10.2136/sssaj2014.05.0190

Brock, O., Kalbitz, K., Absalah, S., & Jansen, B. (2020). Effects of development stage on organic matter transformation in Podzols. *Geoderma*, *378*, 114625. https://doi.org/10.1016/j.geoderma.2020.114625

Burt, R., & Alexander, E. B. (1996). Soil development on moraines of Mendenhall Glacier, southeast Alaska. 2. Chemical transformations and soil micromorphology. *Geoderma*, *72*, 19–36. https://doi.org/10.1016/0016-7061(96)00022-5

Buurman, P., & Jongmans, A. G. (2005). Podzolisation and soil organic matter dynamics. *Geoderma*, *125*, 71–83. https://doi.org/10.1016/j.geoderma.2004.07.006

Carpenter, D. N., Bockheim, J. G., & Reich, P. F. (2014). Soils of temperate rainforests of the North American Pacific Coast. *Geoderma*, *230*, 250–264. https://doi.org/10.1016/j.geoderma.2014.04.023

Carstensen, R., Schoen, J., & Albert, D. (2007). Overview of the biogeographic provinces of southeastern Alaska. In J. Schoen & E. Dovichin (Eds.), *The coastal forests and mountain ecoregion of southeastern Alaska and the Tongass National Forest* (pp. 1–4). Audubon Alaska and the Nature Conservancy. http://www.conservationgateway.org/conservationbygeography/northamerica/unitedstates/alaska/seak/era/cfm/documents/1_introduction.pdf

Catoni, M., D'amico, M. E., Zanini, E., & Bonifacio, E. (2016). Effect of pedogenic processes and formation factors on organic matter stabilization in alpine forest soils. *Geoderma*, *263*, 151–160. https://doi.org/10.1016/j.geoderma.2015.09.005

Chandler, R. F. (1943). The time required for podzol profile formation as evidenced by the Mendenhall Glacial Deposits near Juneau, Alaska. *Soil Science Society of America Journal*, *7*, 454–459. https://doi.org/10.2136/sssaj1943.036159950007000C0077x

Crocker, R. L., & Dickson, B. A. (1957). Soil development on the recessional moraines of the Herbert and Mendenhall Glaciers, South-Eastern Alaska. *Journal of Ecology*, *45*, 169–185. https://doi.org/10.2307/2257083

D'Amore, D. V., Ping, C.-L., & Herendeen, P. A. (2015). Hydromorphic soil development in the coastal temperate rainforest of Alaska. *Soil Science Society of America Journal*, *79*, 698–709. https://doi.org/10.2136/sssaj2014.08.0322

Da Silva, Y. J. A. B., Do Nascimento, C. W. A., Biondi, C. M., Van Straaten, P., De Souza, V. S., & Ferreira, T. O. (2016). Weathering rates and carbon storage along a climosequence of soils developed from contrasting granites in northeast Brazil. *Geoderma*, *284*, 1–12. https://doi.org/10.1016/j.geoderma.2016.08.009

DellaSala, D. A., Alaback, P., Spribille, T., von Wehrden, H., & Nauman, R. S. (2011). Temperate and boreal rainforests of the pacific coast of North America. In D. A. DellaSala (Ed.), *Temperate and boreal rainforests of the world: Ecology and conservation* (pp. 42–81). Island Press.

Edmonds, R. L., & Chappell, H. N. (1994). Relationships between soil organic matter and forest productivity in western Oregon and Washington. *Canadian Journal of Forest Research*, *24*, 1101–1106. https://doi.org/10.1139/x94-146

Eger, A., Almond, P. C., & Condron, L. M. (2012). Upbuilding pedogenesis under active loess deposition in a super-humid, temperate climate — quantification of deposition rates, soil chemistry and pedogenic thresholds. *Geoderma*, *189–190*, 491–501. https://doi.org/10.1016/j.geoderma.2012.06.019

Farr, W. A., & Ford, E. W. (1988). Site quality, forest growth, and soil-site studies in the forests of coastal Alaska. In C. Slaughter & T. Gasbarro (Eds.), *Proceedings of the Alaska Forest Soil Productivity Workshop* (pp. 49–54). USDA Forest Service.

Ford, B., & Brew, D. (1987). Major-element geochemistry of metabasalts of the Juneau-Haines Region, Southeastern Alaska. In J. Galloway & T. Hamilton (Eds.), *Geologic studies in Alaska by the U.S. Geological Survey during 1987* (pp. 150–155). U.S. Geological Survey.

Gannon, J. P., Bailey, S. W., & McGuire, K. J. (2014). Organizing groundwater regimes and response thresholds by soils: A framework for understanding runoff generation in a headwater catchment. *Water Resources Research*, *50*, 8403–8419. https://doi.org/10.1002/2014WR015498

Garcia-Rodeja, E., Silva, B. M., & Macías, F. (1987). Andosols developed from non-volcanic materials in Galicia, NW Spain. *Journal of Soil Science*, *38*, 573–591. https://doi.org/10.1111/j.1365-2389.1987.tb02156.x

Gee, G. W., & Bauder, J. W. (1986). Particle-size analysis. In A. Klute (Ed.), *Methods of soil analysis, part 1: Physical and mineralogical methods* (2nd ed., pp. 383–411). SSSA. https://doi.org/10.2136/sssabookser5.1.2ed.c15

Gehrels, G. E. (2001). Geology of the Chatham Sound region, southeast Alaska and British Columbia. *Canadian Journal of Earth Sciences*, *38*, 1579–1599. https://doi.org/10.1139/e01-040

Gehrels, G. E., & Berg, H. C. (1994). Geology of southeastern Alaska. *Geological Society of America*, *1*, 451–467.

Goldich, S. S. (1938). A study in rock-weathering. *Journal of Geology*, *46*, 17–58. https://doi.org/10.1086/624619

Goldin, A., & Edmonds, J. (1996). A numerical evaluation of some Florida Spodosols. *Physical Geography*, *17*, 242–252. https://doi.org/10.1080/02723646.1996.10642583

Goldthwait, R. P., Loewe, F., Ugolini, F. C., Decker, H. F., DeLong, D. M., Trautman, M. B., Good, E. E., Merrell III, T. R., & Rudolph, E. D. (1966). *Soil development and ecological succession in a deglaciated area of Muir inlet, southeast Alaska* (Institute of Polar Studies Report No. 20). Goldthwait Polar Library.

Griscom, B. W., Adams, J., Ellis, P. W., Houghton, R. A., Lomax, G., Miteva, D. A., Schlesinger, W. H., Shoch, D., Siikamäki, J. V., Smith, P., Woodbury, P., Zganjar, C., Blackman, A., Campari, J., Conant, R. T., Delgado, C., Elias, P., Gopalakrishna, T., Hamsik, M. R., … Fargione, J. (2017). Natural climate solutions. *PNAS*, *114*, 11645–11650. https://doi.org/10.1073/pnas.1710465114

Harden, J. W. (1982). A quantitative index of soil development from field descriptions: Examples from a chronosequence in central California. *Geoderma*, *28*, 1–28. https://doi.org/10.1016/0016-7061(82)90037-4

Harden, J. W., & Taylor, E. M. (1983). A quantitative comparison of soil development in four climatic regimes. *Quaternary Research*, *20*, 342–359. https://doi.org/10.1016/0033-5894(83)90017-0

Harper, R. J., & Tibbett, M. (2013). The hidden organic carbon in deep mineral soils. *Plant and Soil*, *368*, 641–648. https://doi.org/10.1007/s11104-013-1600-9

Harrison, R. B., Footen, P. W., & Strahm, B. D. (2011). Deep soil horizons: Contribution and importance to soil carbon pools and in assessing whole-ecosystem response to management and global change. *Forest Science*, *57*, 67–76.

Heckman, K., Lawrence, C. R., & Harden, J. W. (2018). A sequential selective dissolution method to quantify storage and stability of organic carbon associated with Al and Fe hydroxide phases. *Geoderma*, *312*, 24–35. https://doi.org/10.1016/j.geoderma.2017.09.043

Heckman, K., Welty-Bernard, A., Rasmussen, C., & Schwartz, E. (2009). Geologic controls of soil carbon cycling and microbial dynamics in temperate conifer forests. *Chemical Geology*, *267*, 12–23. https://doi.org/10.1016/j.chemgeo.2009.01.004

Heilman, P. E., & Gass, C. R. (1974). Parent materials and chemical properties of mineral soils in southeast Alaska. *Soil Science*, *117*, 21–27. https://doi.org/10.1097/00010694-197401000-00003

Heusser, C. J. (1960). *Late-pleistocene environments of North Pacific North America: An elaboration of late-glacial and postglacial climactic, physiographic, and biotic changes*. American Geographical Society.

Homann, P. S., Remillard, S. M., Harmon, M. E., & Bormann, B. T. (2004). Carbon storage in coarse and fine fractions of pacific northwest old-growth forest soils. *Soil Science Society of America Journal*, *68*, 2023–2030. https://doi.org/10.2136/sssaj2004.2023

Iamarino, M., & Terribile, F. (2008). The importance of andic soils in mountain ecosystems: A pedological investigation in Italy. *European Journal of Soil Science*, *59*, 1284–1292. https://doi.org/10.1111/j.1365-2389.2008.01075.x

IPCC. (2021). Summary for policymakers. In V. Masson-Delmotte, P. Zhai, A. Pirani, S. L. Connors, C. Péan, S. Berger, N. Caud, Y. Chen, L. Goldfarb, M. I. Gomis, M. Huang, K. Leitzell, E. Lonnoy, J. B. R. Matthews, T. K. Maycock, T. Waterfield, O. Yelekçi, R. Yu, & B. Zhou (Eds.), *Climate change 2021: The physical science basis. Contribution of working group I to the sixth assessment report of the Intergovernmental Panel on Climate Change*. Cambridge University Press. https://www.ipcc.ch/report/ar6/wg1/

Jackson, M. L., Hseung, Y., Corey, R. B., Evans, E. J., & Heuvel, R. C. V (1952). Weathering sequence of clay-size minerals in soils and sediments. *Soil Science Society of America Journal*, *16*, 3–6. https://doi.org/10.2136/sssaj1952.03615995001600010002x

James, J., Devine, W., Harrison, R., & Terry, T. (2014). Deep soil carbon: Quantification and modeling in subsurface layers. *Soil Science Society of America*, *78*, S1–S10. https://doi.org/10.2136/sssaj2013.06.0245nafsc

Johnson, D. W., Murphey, J. D., Rau, B. M., & Miller, W. (2011). Subsurface carbon contents: Some case studies in forest soils. *Forest Science*, *57*, 3–10.

Johnson, K. D., Harden, J., Mcguire, A. D., Bliss, N. B., Bockheim, J. G., Clark, M., Nettleton-Hollingsworth, T., Jorgenson, M. T., Kane, E. S., Mack, M., O'Donnell, J., Ping, C.-L., Schuur, E. A. G., Turetsky, M. R., & Valentine, D. W. (2011). Soil carbon distribution in Alaska in relation to soil-forming factors. *Geoderma*, *167–168*, 71–84. https://doi.org/10.1016/j.geoderma.2011.10.006

Kalbitz, K., Solinger, S., Park, J.-H., Michalzik, B., & Matzner, E. (2000). Controls on the dynamics of dissolved organic matter in soils: A review. *Soil Science*, *165*, 277–304. https://doi.org/10.1097/00010694-200004000-00001

Keith, H., Mackey, B. G., & Lindenmayer, D. B. (2009). Re-evaluation of forest biomass carbon stocks and lessons from the world's most carbon-dense forests. *PNAS*, *106*(28), 11635–11640. https://doi.org/10.1073/pnas.0901970106

Kleber, M., Bourg, I. C., Coward, E. K., Hansel, C. M., Myneni, S. C. B., & Nunan, N. (2021). Dynamic interactions at the mineral–organic matter interface. *Nature Reviews Earth & Environment*, *2*, 402–421. https://doi.org/10.1038/s43017-021-00162-y

Kleber, M., Mikutta, R., Torn, M. S., & Jahn, R. (2005). Poorly crystalline mineral phases protect organic matter in acid subsoil horizons. *European Journal of Soil Science*, *56*, 717–725. https://doi.org/10.1111/j.1365-2389.2005.00706.x

Kögel-Knabner, I., & Amelung, W. (2021). Soil organic matter in major pedogenic soil groups. *Geoderma*, *384*, 114785. https://doi.org/10.1016/j.geoderma.2020.114785

Kögel-Knabner, I., Guggenberger, G., Kleber, M., Kandeler, E., Kalbitz, K., Scheu, S., Eusterhues, K., & Leinweber, P. (2008). Organo-mineral associations in temperate soils: Integrating biology, mineralogy, and organic matter chemistry. *Journal of Plant Nutrition and Soil Science*, *171*, 61–82. https://doi.org/10.1002/jpln.200700048

Konen, M. E., Burras, C. L., & Sandor, J. A. (2003). Organic carbon, texture, and quantitative color measurement relationships for cultivated soils in north central Iowa. *Soil Science Society of America Journal*, *67*, 1823–1830. https://doi.org/10.2136/sssaj2003.1823

Krettek, A., Herrmann, L., & Rennert, T. (2020). Podzolisation affects the spatial allocation and chemical composition of soil organic matter fractions. *Soil Research*, *58*, 713–725. https://doi.org/10.1071/SR20164

Leighty, W. W., Hamburg, S. P., & Caouette, J. (2006). Effects of management on carbon sequestration in forest biomass in southeast Alaska. *Ecosystems*, *9*, 1051–1065. https://doi.org/10.1007/s10021-005-0028-3

Lewis, T. (1976). *The till—Derived podzols of Vancouver Island* [PhD dissertation, The University of British Columbia].

Lin, H. (2012). *Hydropedology: synergistic integration of soil science and hydrology* (1st ed.). Academic Press.

Littke, K. M., Harrison, R. B., Briggs, D. G., & Grider, A. R. (2011). Understanding soil nutrients and characteristics in the Pacific Northwest through parent material origin and soil nutrient regimes. *Canadian Journal of Forest Research*, *41*, 2001–2008. https://doi.org/10.1139/x11-115

Lundström, U., van Breemen, N., & Bain, D. (2000). The podzolization process: A review. *Geoderma*, *94*, 91–107. https://doi.org/10.1016/S0016-7061(99)00036

Lybrand, R. A., & Rasmussen, C. (2015). Quantifying climate and landscape position controls on soil development in semiarid ecosystems. *Soil Science Society of America Journal*, *79*, 104–116. https://doi.org/10.2136/sssaj2014.06.0242

Macyk, T. M., Lindsay, J. D., & Pawluk, S. (1978). Relief and microclimate as related to soil properties. *Canadian Journal of Soil Science*, *58*, 421–438. https://doi.org/10.4141/cjss78-049

Matus, F., Rumpel, C., Neculman, R., Panichini, M., & Mora, M. L. (2014). Soil carbon storage and stabilisation in andic soils: A review. *CATENA*, *120*, 102–110. https://doi.org/10.1016/j.catena.2014.04.008

McClelland, W. C., Gehrels, G. E., Samson, S. D., & Patchett, P. J (1992). Protolith relations of the Gravina Belt and Yukon-Tanana terrane in central southeastern Alaska. *Journal of Geology*, *100*, 107–123. https://doi.org/10.1086/629574

McKeague, J. A., DeConinck, F., & Franzmeier, D. P. (1983). Spodosols. In L. P. Wilding, N. E. Smeck, & G. F. Hall (Eds.), *Pedogenesis and soil taxonomy* (pp. 217–252). Elsevier.

McNicol, G., Bulmer, C., D'amore, D., Sanborn, P., Saunders, S., Giesbrecht, I., Arriola, S. G., Bidlack, A., Butman, D., & Buma, B. (2019). Large, climate-sensitive soil carbon stocks mapped with pedology-informed machine learning in the north pacific coastal temperate rainforest. *Environmental Research Letters*, *14*, 1–12. https://doi.org/10.1088/1748-9326/aaed52

Mikutta, R., Kleber, M., Kaiser, K., & Jahn, R. (2005). Review: Organic matter removal from soils using hydrogen peroxide, sodium hypochlorite, and sodium peroxodisulfate. *Soil Science Society of America Journal*, *69*, 120–135. https://doi.org/10.2136/sssaj2005.0120

Mileti, F. A., Vingiani, S., Manna, P., Langella, G., & Terribile, F. (2017). An integrated approach to studying the genesis of Andic soils in Italian non-volcanic mountain ecosystems. *Catena*, *159*, 35–50. https://doi.org/10.1016/j.catena.2017.07.022

Miller, D. C., & Birkeland, P. W. (1992). Soil catena variation along an alpine climatic transect, northern Peruvian Andes. *Geoderma*, *55*, 211–223. https://doi.org/10.1016/0016-7061(92)90084-K

Musielok, Ł., Buczek, K., & Karcz, T. (2022). Relief-induced feedback mechanisms controlling local podzolization occurrence on flysch slopes—Examples from Outer Western Carpathians (southern Poland). *Catena*, *213*, 106124. https://doi.org/10.1016/j.catena.2022.106124

Musielok, Ł., Drewnik, M., Szymański, W., Stolarczyk, M., Gus-Stolarczyk, M., & Skiba, M. (2021). Conditions favoring local podzolization in soils developed from flysch regolith—A case study from the Bieszczady mountains in southeastern Poland. *Geoderma*, *381*, 114667. https://doi.org/10.1016/j.geoderma.2020.114667

Nave, L. E., Bowman, M., Gallo, A., Hatten, J. A., Heckman, K. A., Matosziuk, L., Possinger, A. R., Sanclements, M., Sanderman, J., Strahm, B. D., Weiglein, T. L., & Swanston, C. W. (2021). Patterns and predictors of soil organic carbon storage across a continental-scale network. *Biogeochemistry*, *156*, 75–96. https://doi.org/10.1007/s10533-020-00745-9

Pan, Y., Birdsey, R. A., Phillips, O. L., & Jackson, R. B. (2013). The structure, distribution, and biomass of the world's forests. *Annual Review of Ecology and Systematics*, *44*, 593–622. https://doi.org/10.1146/annurev-ecolsys-110512-135914

Patton, N. R., Lohse, K. A., Seyfried, M. S., Godsey, S. E., & Parsons, S. B. (2019). Topographic controls of soil organic carbon on soil-mantled landscapes. *Scientific Reports*, *9*, 6390. https://doi.org/10.1038/s41598-019-42556-5

R Core Team. (2020). *R: A language and environment for statistical computing*. R Foundation for Statistical Computing. https://www.R-project.org/

Rasmussen, C. (2006). Distribution of soil organic and inorganic carbon pools by biome and soil taxa in Arizona. *Soil Science Society of America Journal*, *70*, 256–265. https://doi.org/10.2136/sssaj2005.0118

Rasmussen, C., Heckman, K., Wieder, W. R., Keiluweit, M., Lawrence, C. R., Berhe, A. A., Blankinship, J. C., Crow, S. E., Druhan, J. L., Hicks Pries, C. E., Marin-Spiotta, E., Plante, A. F., Schädel, C., Schimel, J. P., Sierra, C. A., Thompson, A., & Wagai, R. (2018). Beyond clay: Towards an improved set of variables for predicting soil organic matter content. *Biogeochem*, *137*, 297–306. https://doi.org/10.1007/s10533-018-0424-3

Rumpel, C., & Kögel-Knabner, I. (2011). Deep soil organic matter—A key but poorly understood component of terrestrial C cycle. *Plant and Soil*, *338*, 143–158. https://doi.org/10.1007/s11104-010-0391-5

Sanborn, P., Lamontagne, L., & Hendershot, W. (2011). Podzolic soils of Canada: Genesis, distribution, and classification. *Canadian Journal of Soil Science*, *91*, 843–880. https://doi.org/10.4141/cjss10024

Sauer, D., Sponagel, H., Sommer, M., Giani, L., Jahn, R., & Stahr, K. (2007). Podzol: Soil of the year 2007. A review on its genesis, occurrence, and functions. *Journal of Plant Nutrition and Soil Science*, *170*, 581–597. https://doi.org/10.1002/jpln.200700135

Schaetzl, R. J. (1991a). Factors affecting the formation of dark, thick epipedons beneath forest vegetation, Michigan, USA. *Journal of Soil Science*, *42*, 501–512. https://doi.org/10.1111/j.1365-2389.1991.tb00426.x

Schaetzl, R. J. (1991b). A lithosequence of soils in extremely gravelly, dolomitic parent materials, Bois Blanc Island, Lake Huron. *Geoderma*, *48*, 305–320. https://doi.org/10.1016/0016-7061(91)90050-4

Schaetzl, R., & Harris, W. (2012). Spodosols. In P. M. Huang, Y. Li, & M. E. Sumner (Eds.), *Handbook of soil sciences: Properties and processes* (2nd ed.). CRC Press. https://doi.org/10.1201/b11267

Schaetzl, R. J., & Isard, S. A. (1991). The distribution of spodosol soils in southern Michigan: A climatic interpretation. *Annals of the American Association of Geographers*, *81*, 425–442. https://doi.org/10.1111/j.1467-8306.1991.tb01703.x

Schaetzl, R. J., Mikesell, L. R., & Velbel, M. A. (2006). Soil characteristics related to weathering and pedogenesis across a geomorphic surface of uniform age in Michigan. *Physical Geography*, *27*, 170–188. https://doi.org/10.2747/0272-3646.27.2.170

Schaetzl, R. J., & Mokma, D. L. (1988). A numerical index of podzol and podzolic soil development. *Physical Geography*, *9*(3), 232–246. https://doi.org/10.1080/02723646.1988.10642352

Schaetzl, R. J., & Thompson, M. L. (2015). *Soils: Genesis and geomorphology* (2nd ed.). Cambridge University Press.

Scharlemann, J. P., Tanner, E. V., Hiederer, R., & Kapos, V. (2014). Global soil carbon: Understanding and managing the largest terrestrial carbon pool. *Carbon Management*, *5*, 81–91. https://doi.org/10.4155/cmt.13.77

Schoeneberger, P. J., Wysocki, D. A., Benham, E. C., & Soil Survey Staff. (2021). *Field book for describing and sampling soils* (Version 3.0). National Soil Survey Center, NRCS, USDA. (Original work published in 2012). https://www.nrcs.usda.gov/sites/default/files/2022-09/field-book.pdf

Schulze, K., Borken, W., Muhr, J., & Matzner, E. (2009). Stock, turnover time and accumulation of organic matter in bulk and density fractions of a Podzol soil. *European Journal of Soil Science*, *60*, 567–577. https://doi.org/10.1111/j.1365-2389.2009.01134.x

Semmel, A., & Terhorst, B. (2010). The concept of the Pleistocene periglacial cover beds in central Europe: A review. *Quaternary International*, *222*, 120–128. https://doi.org/10.1016/j.quaint.2010.03.010

Sharma, P. V. (1997). *Environmental and engineering geophysics*. Cambridge University Press. https://doi.org/10.1017/CBO9781139171168.002

Slessarev, E. W., Lin, Y., Bingham, N. L., Johnson, J. E., Dai, Y., Schimel, J. P., & Chadwick, O. A. (2016). Water balances creates a threshold in soil pH at the global scale. *Nature*, *540*, 567–569. https://doi.org/10.1038/nature20139

Smithwick, E. A. H., Harmon, M. E., Remillard, S. M., Acker, S. A., & Franklin, J. F. (2002). Potential upper bounds of carbon stores in forests of the Pacific Northwest. *Ecological Society of America*, *12*, 1303–1317. https://doi.org/10.1890/1051-0761(2002)012(1303:PUBOCS)2.0.CO2

Soil Survey Staff. (2013). *Soil Series Classification Database*. USDA-NRCS. http://soils.usda.gov/technical/classification/

Soil Survey Staff. (2014). *Soil survey field and laboratory methods manual* (Soil survey investigations report No. 51). USDA-NRCS.

Soil Survey Staff. (2022). *Gridded National Soil Survey Geographic (gNATSGO) database for the conterminous United States*. USDA-NRCS. https://www.nrcs.usda.gov/wps/portal/nrcs/detail/soils/survey/geo/?cid=nrcseprd1464625#distribution

Sommer, M., Halm, D., Geisinger, C., Andruschkewitsch, I., Zarei, M., & Stahr, K. (2001). Laterial pedolizaiton in a sandstone catchment. *Geoderma*, *103*, 231–247. https://doi.org/10.1016/S0016-7061(01)00018-0

Spinola, D., Portes, R., Fedenko, J., Lybrand, R., Dere, A., Biles, F., Trainor, T., Bowden, M. E., & D'amore, D. (2022). Lithological controls on soil geochemistry and clay mineralogy across Spodosols in the coastal temperate rainforest of southeast Alaska. *Geoderma*, *428*, 116211. https://doi.org/10.1016/j.geoderma.2022.116211

Sposito, G., Skipper, N. T., Sutton, R., Park, S.-H., Soper, A. K., & Greathouse, J. A. (1999). Surface geochemistry of the clay minerals. *PNAS*, *96*, 3358–3364. https://doi.org/10.1073/pnas.96.7.3358

Stone, E. L., Harris, W. G., Brown, R. B., & Kuehl, R. J. (1993). Carbon storage in Florida Spodosols. *Soil Science Society of America Journal*, *57*, 179–182. https://doi.org/10.2136/sssaj1993.03615995005700010032x

Stowell, H. H. (1990). Structural development of the western metamorphic belt adjacent to the coast plutonic complex, southeastern Alaska: Evidence from Holkham Bay. *Tectonics*, *9*, 391–407.

Tan, Z., Lal, R., Smeck, N. E., Calhoun, F. G., Slater, B. K., Parkinson, B., & Gehring, R. M. (2004). Taxonomic and geographic distribution of soil organic carbon pools in Ohio. *Soil Science Society of America Journal*, *68*, 1896–1904. https://doi.org/10.2136/sssaj2004.1896

Terribile, F., Iamarino, M., Langella, G., Manna, P., Mileti, F. A., Vingiani, S., & Basile, A. (2018). The hidden ecological resource of andic soils in mountain ecosystems: evidence from Italy. *Solid Earth*, *9*(1), 63–74. https://doi.org/10.5194/se-9-63-2018

Torri, D., Poesen, J., Monaci, F., & Busoni, E. (1994). Rock fragment content and fine soil bulk density. *Catena*, *23*, 65–71. https://doi.org/10.1016/0341-8162(94)90053-1

U.S. Forest Carbon Data. (2023). *U.S. Forest carbon data: In brief*. Congressional Research Service. https://fas.org/sgp/crs/misc/R46313.pdf

USDA Forest Service. (1996). *A landform classification guide for the Alaska region: Classification guide*. USDA Forest Service. https://www.fs.usda.gov/Internet/FSE_DOCUMENTS/stelprdb5416185.pdf

USDA Forest Service. (2016). *Tongass National Forest Land and resource management plan*. https://www.fs.usda.gov/Internet/FSE_DOCUMENTS/fseprd527907.pdf

Ussiri, D. A. N., & Johnson, C. E. (2004). Sorption of organic carbon fractions by Spodosol mineral horizons. *Soil Science Society of America Journal*, *68*, 253–262. https://doi.org/10.2136/sssaj2004.0253

Valerio, M. W., Mcdaniel, P. A., & Gessler, P. E. (2016). Distribution and properties of podzolized soils in the northern Rocky Mountains. *Soil Science Society of America Journal*, *80*, 1308–1316. https://doi.org/10.2136/sssaj2016.04.0109

Vejre, H., Callesen, I., Vesterdal, L., & Raulund-Rasmussen, K. (2003). Carbon and nitrogen in Danish forest soils-contents and distribution determined by soil order. *Soil Science Society of America Journal*, *67*, 335–343. https://doi.org/10.2136/sssaj2003.0335

Viereck, L. A., Dyrness, C. T., Batten, A. R., & Wenzlick, K. J. (1992). *The Alaska vegetation classification* (General technical report, PNW-GTR-286). USDA Forest Service, Pacific Northwest Research Station.

Wei, Y., Li, M., Chen, H., Lewis, B. J., Yu, D., Zhou, L., Zhou, W., Fang, X., Zhao, W., & Dai, L. (2013). Variation in carbon storage and its distribution by stand age and forest type in boreal and temperate forests in northeastern China. *PLoS One*, *8*, 72201. https://doi.org/10.1371/journal.pone.0072201

Wilson, P. (2001). Rate and nature of podzolisation in aeolian sands in the Falkland Islands, South Atlantic. *Geoderma*, *101*, 77–86. https://doi.org/10.1016/S0016-7061(00)00091-4

Zhu, M., Feng, Q., Qin, Y., Cao, J., Zhang, M., Liu, W., Deo, R. C., Zhang, C., Li, R., & Li, B. (2019). The role of topography in shaping the spatial patterns of soil organic carbon. *CATENA*, *176*, 296–305. https://doi.org/10.1016/j.catena.2019.01.029

SUPPORTING INFORMATION

Additional supporting information can be found online in the Supporting Information section at the end of this article.

How to cite this article: Fedenko, J., D'Amore, D., Spinola, D., Portes, R., Dere, A., & Lybrand, R. A. (2024). Spodosol development and soil organic carbon distribution along a lithosequence in perhumid coastal temperate rainforest. *Soil Science Society of America Journal*, *88*, 1509–1528. https://doi.org/10.1002/saj2.20695